

UNCLASSIFIED

AD NUMBER
AD840087
NEW LIMITATION CHANGE
TO Approved for public release, distribution unlimited
FROM Distribution authorized to U.S. Gov't. agencies and their contractors; Critical Technology; AUG 1968. Other requests shall be referred to Air Force Flight Dynamics Laboratory, ATTN: FDFM, Wright-Patterson AFB, OH 45433.
AUTHORITY
AFFDL ltr dtd 27 Aug 1973

THIS PAGE IS UNCLASSIFIED

AD 340087

ANALYTICAL LANDING GEAR – SOILS INTERACTION – PHASE I

DAVID C. KRAFT

*University of Dayton
Research Institute*

TECHNICAL REPORT AFFDL-TR-68-88

AUGUST 1968

This document is subject to special export controls and each transmittal to foreign governments or foreign nationals may be made only with prior approval of the Air Force Flight Dynamics Laboratory (FDFM), Wright-Patterson Air Force Base, Ohio 45433.

AIR FORCE FLIGHT DYNAMICS LABORATORY
AIR FORCE SYSTEMS COMMAND
WRIGHT-PATTERSON AIR FORCE BASE, OHIO

NOTICE

When Government drawings, specifications, or other data are used for any purpose other than in connection with a definitely related Government procurement operation, the United States Government thereby incurs no responsibility nor any obligation whatsoever; and the fact that the Government may have formulated, furnished, or in any way supplied the said drawings, specifications, or other data, is not to be regarded by implication or otherwise as in any manner licensing the holder or any other person or corporation, or conveying any rights or permission to manufacture, use, or sell any patented invention that may in any way be related thereto.

This document is subject to special export controls and each transmittal to foreign governments or foreign nationals may be made only with prior approval of the Air Force Flight Dynamics Laboratory (FDFM), Wright-Patterson Air Force Base, Ohio 45433. The reason for this distribution limitation is that the report would enhance Sino-Soviet bloc military and industrial research programs having a potential strategic value.

COPIES

DATE OF COPY

DATE OF ISSUE

BY

DISTRIBUTION/AVAILABILITY

DIST.	AVAIL.	STG.	S.
2			

Copies of this report should not be returned unless return is required by security considerations, contractual obligations, or notice on a specific document.

AFFDL-TR-68-88

**ANALYTICAL LANDING GEAR – SOILS
INTERACTION – PHASE I**

DAVID C. KRAFT

This document is subject to special export controls and each transmittal to foreign governments or foreign nationals may be made only with prior approval of the Air Force Flight Dynamics Laboratory (FFDL), Wright-Patterson Air Force Base, Ohio 45433.

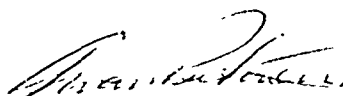
FOREWORD

The contract was initiated under Project No. 1369, "Mechanical Subsystems," Task No. 136908, "Landing Gear And Alighting Shock Absorption Systems And Aircraft Flotation." Accomplishment of this effort was made possible wholly through the use of Laboratory Director's Fund. This report was prepared by the Aerospace Mechanics Group of the University of Dayton Research Institute under USAF Contract AF 33(615)-3199. The work was conducted under the direction of the Vehicle Equipment Division, Air Force Flight Dynamics Laboratory, Wright-Patterson Air Force Base, Ohio, Mr. George Sperry (FDFM), Project Engineer.

This report covers work conducted from 15 May 1967 to 15 May 1968.

The author wishes to thank Mr. Sperry for providing considerable insight and information related to specific Air Force requirements for forward area aircraft operations, and to Mr. Edward Pekarek for his assistance in programming the dynamic response solution. This report was submitted by the author in May 1968.

Publication of this technical report does not constitute Air Force approval of the report's findings or conclusions. It is published only for the exchange and stimulation of ideas.



AIVARS V. PETERSONS
Acting Chief, Mechanical Branch
Vehicle Equipment Division
Air Force Flight Dynamics Laboratory

ABSTRACT

The determination of aircraft flotation and operation capability on semi- and unprepared soil runways is a critical factor in developing forward area airfields in limited warfare situations. An investigation was conducted to determine the variables which significantly influence aircraft performance when operating on soil runways.

Analysis of available experimental drag-sinkage-velocity data led to the defining of at least three distinct regions for which the sinkage ratio-velocity relationship shows a distinct response. A drag ratio-sinkage ratio equation was developed for use in one of these velocity regions. The effects of twin wheel and tandem wheel arrangements were analyzed on a preliminary basis. The results of a sinkage study using presently available sinkage prediction equations indicated that present sinkage analysis accuracy is in the range of $\pm 50\%$ to $\pm 100\%$.

In order to develop a suitable flotation criteria, an investigation was conducted of the dynamic landing gear contacting element-soil interaction response utilizing elastic theory. These results led to the development of a flotation parameter (related to sinkage) and a flotation index (related to drag) in nomographic form which permits comparative flotation analysis of landing gear systems.

This document is subject to special export controls and each transmittal to foreign governments or foreign nationals may be made only with prior approval of the Air Force Flight Dynamics Laboratory (AFFDL), Wright-Patterson Air Force Base, Ohio 45433. The reason for this distribution limitation is that the report would enhance Sino-Soviet bloc military and industrial research programs having a potential strategic value.

TABLE OF CONTENTS

SECTION	PAGE
I INTRODUCTION	1
II IDENTIFICATION OF VARIABLES	3
III DRAG-SINKAGE EQUATIONS	7
IV SINKAGE PREDICTION ANALYSIS	20
V FLOTATION PARAMETER	34
VI AIRCRAFT OPERATION CAPABILITY (SUITABILITY OF SITE)	46
VII CONCLUSIONS AND RECOMMENDATIONS FOR RESEARCH	51
REFERENCES	53
APPENDIX I Drag-Sinkage Experimental Data	56
APPENDIX II Transient Loading Sinkage Analysis, Computer Program	64

ILLUSTRATIONS

Figure		Page
1	Aircraft Tire Sinkage	2
2	Variables in Landing Gear-Unprepared Runway Problem	5
3	Wheel-Ground Interaction	8
4	Drag Ratio vs Horizontal Velocity on Soil	10
5	Drag Ratio-Sinkage Ratio, Single Wheel on Soil	13
6	Drag Ratio-Sinkage Ratio, Single Wheel WES Data on Soil	16
7	Drag Ratio-Sinkage Ratio, Twin Wheel WES Data on Soil	17
8	Drag Ratio-Sinkage Ratio, Multiple Wheel WES Data on Soil	18
9	Sinkage Ratio vs Wheel Load, 20.00-20 Tire, $d = 33\text{-}1/3\%$ on Sand Soil, $G = 5, 10, 20$	26
10	Sinkage Ratio vs Tire Deflection, 20.00-20 Tire, $P = 6000$ lbs on Sand Soil	27
11	Sinkage Ratio vs Tire Width, 50 inch Diameter Tire, $P = 6000$ lbs on Sand Soil	28
12	Sinkage Ratio vs Wheel Load, 20.00-20 Tire, $d = 33\text{-}1/3\%$ on Clay Soil, $CBR = 2, 5$	30
13	Sinkage Ratio vs Tire Deflection, 20.00-20 Tire, $P = 16,000$ lbs. on Clay Soil	32
14	Normalized Tire Deflection vs Contact Area Ratio	36
15	Load-Time History in Soil Due to Moving Wheel	38
16	Half Space Mathematical Model (Elastic System)	40
17	Flotation Parameter Nomograph	42
18	CBR Required for Operation of Aircraft on Unsurfaced Soils	47
19	Equivalent Single-Wheel Load Adjustment Curve for Unsurfaced Soils	48
20	Unified Approach: Flotation Parameter-Aircraft Operation Capability	50
21	Periodic Loading Pulses	68
22	Dimensionless Loading Function (Half Sine Wave)	68

LIST OF TABLES

	Page
I Significant Variables: Soil, Landing Gear Tires	3
II Drag Variables	7
III Elliptical Contact Geometry	35
IV Influence of Component Loading on Sinkage	37
V Velocity-Duration Relationship	39
VI Drag-Sinkage Data, Reference (8), Single Wheel	57
VII Drag-Sinkage Data, Reference (2), Single Wheel	58
VIII Drag-Sinkage Data, Reference (3), Single Wheel	59
IX Drag-Sinkage Data, Reference (7), Single Wheel	60
X Drag-Sinkage Data, Reference (7), Twin Wheel	61
XI Drag-Sinkage Data, Reference (7), Multiple Wheel	62
XII Drag-Sinkage Data, Reference (5), Single Wheel	63
XIII Dimensionless Parameters - Uniform Loading Case	70

LIST OF SYMBOLS

A	Tire contact area
A_1, A_2	Tire contact areas corresponding to tire deflections d_1 and d_2 , respectively
a	Major axis of ellipse
a_n	Fourier series coefficient
a_o	Dimensionless frequency ratio
a_{on}	Frequency ratio corresponding to n-index
B	Mass ratio
b	Tire width and Minor axis of ellipse
b_n	Fourier series coefficient
C_{DI}	Impingement drag coefficient related to soil
CBR	California Bearing Ratio
CI	Cone Index
CMN	Clay Mobility Number
c	Cohesion of soil
c_1	Dimensionless damping coefficient
c_{1n}	Damping coefficient corresponding to n-index
c_n	Fourier series coefficient
D	Tire diameter
D'	Additional drag due to soil inertia effects
D_y	Dynamic factor related to duration of loading
d	Tire deflection in per cent
d_1, d_2	Tire deflections corresponding to tire contact areas A_1 and A_2 respectively
e	Base of natural logarithms
F	Flotation parameter based on sinkage
F_1, F_2	Parameters in complex displacement function
F.I.	Flotation Index based on drag
f	Coefficient related to tire type
f	Functional expression
f_1, f_2	Parameters in complex displacement function
G	Shear modulus of soil and Slope of cone index versus depth curve
g	Acceleration of gravity

H	Height of bow wave
h_t	Tire section height
i	$\sqrt{-1}$ and Summation index
j	Integer used to control the period of the impulse
K	Constant in high velocity drag equation related to soil density and tire width
K_1, K_2	Constants
K_s	Coefficient of subgrade reaction
k	Spring constant
k_c	Soil deformation modulus
k_d	Instantaneous dynamic soil spring rate
k_s	Static soil spring rate
k_1	Dimensionless spring constant
k_{1n}	Spring constant corresponding to n-index
k_ϕ	Soil deformation modulus
l, l_1	Footprint length
M	Magnification factor and Number of intervals used to define the pulse shape
M_n	Magnification factor corresponding to n-index
m	Equivalent mass of gear-wheel
N	Large integer
n	Exponent of sinkage and Subscript index
P	Vertical load
$P(t)$	Time dependent vertical load function
PR	Ply rating
P_o	Peak amplitude of force function, $P(t)$
p	Contact stress
p_c	Carcass pressure
p_i	Inflation pressure
p_m	Maximum bearing strength
R	Drag magnitude
r	Radius of CBR piston
r_o	Radius of circularly loaded area

S	Slip ratio
SMN	Sand Mobility Number
T	Aircraft thrust
t	Time
t_d	Time duration of load pulse
u	Dimensionless time variable
V	Horizontal velocity
V_s	Shear wave velocity in soil
w_e	Elastic part of total sinkage
w_p	Plastic part of total sinkage
Y_i	Amplitude of load shape function
Z	Instantaneous sinkage of tire into soil
Z(t)	Time dependent sinkage function
Z_m	Sinkage at maximum bearing strength
δ_t	Tire deflection
ϵ	Constant used to define the accuracy of the numerical evaluation
η	Soil viscosity
λ	Coefficient of friction, tire to soil
μ	Poisson's ratio
π	3.1416
ρ	Soil density
ϕ	Phase shift between sinkage and loading function
ϕ_n	Phase shift corresponding to n-index
$\phi(t/t_d)$	Dimensionless load pulse shape function
ψ_n	Phase relationship between the individual frequency components
ω	Angular frequency
ω_n	Angular frequency corresponding to n-index

SECTION I

INTRODUCTION

The conduction of limited warfare in many cases requires the operation of aircraft on forward area semi- and unprepared soil surfaces. The effective and efficient utilization of aircraft demands that landings on, maneuvers on, and takeoff from minimum length and width soil surfaces be accomplished with maximum aircraft control and safety at maximum loads with the smallest possible deterioration and damage to the aircraft and airfield surface.

Since of necessity these forward airfields are limited in ground strength and runway length, aircraft landing gear sinkage, ground drag, and surface roughness are critical factors to the utilization of soil surfaced airfields. An indication of the magnitudes of sinkage is shown in Figure 1. Currently available flotation criteria and analysis is based on empirical results of full scale experimental tests conducted with only limited ranges of such variables as load, tire parameters, landing gear configuration, and soil conditions.

The basic objective of this program is to analytically define landing gear - soil surface interaction in order to establish adequate aircraft flotation criteria. This objective is to be accomplished by a three phase program. Phase I, described in this report, included a determination of the critical parameters affecting flotation, an investigation of available experimental data and analyses for defining landing gear sinkage, surface drag, and the interrelationship between sinkage and drag leading to the development of a suitable mathematical model for establishing flotation criteria.

Phase II is concerned with the development of analysis equations for use with computer simulation techniques to analytically define the range of variables associated with flotation. Initial development will be made of a sinkage and drag index for defining aircraft flotation in nomographic form. In Phase III the effects of braking, high velocity, and multiple wheel effects will be analyzed leading to the development of a final flotation criteria for defining aircraft performance on semi- and unprepared soil airstrips.

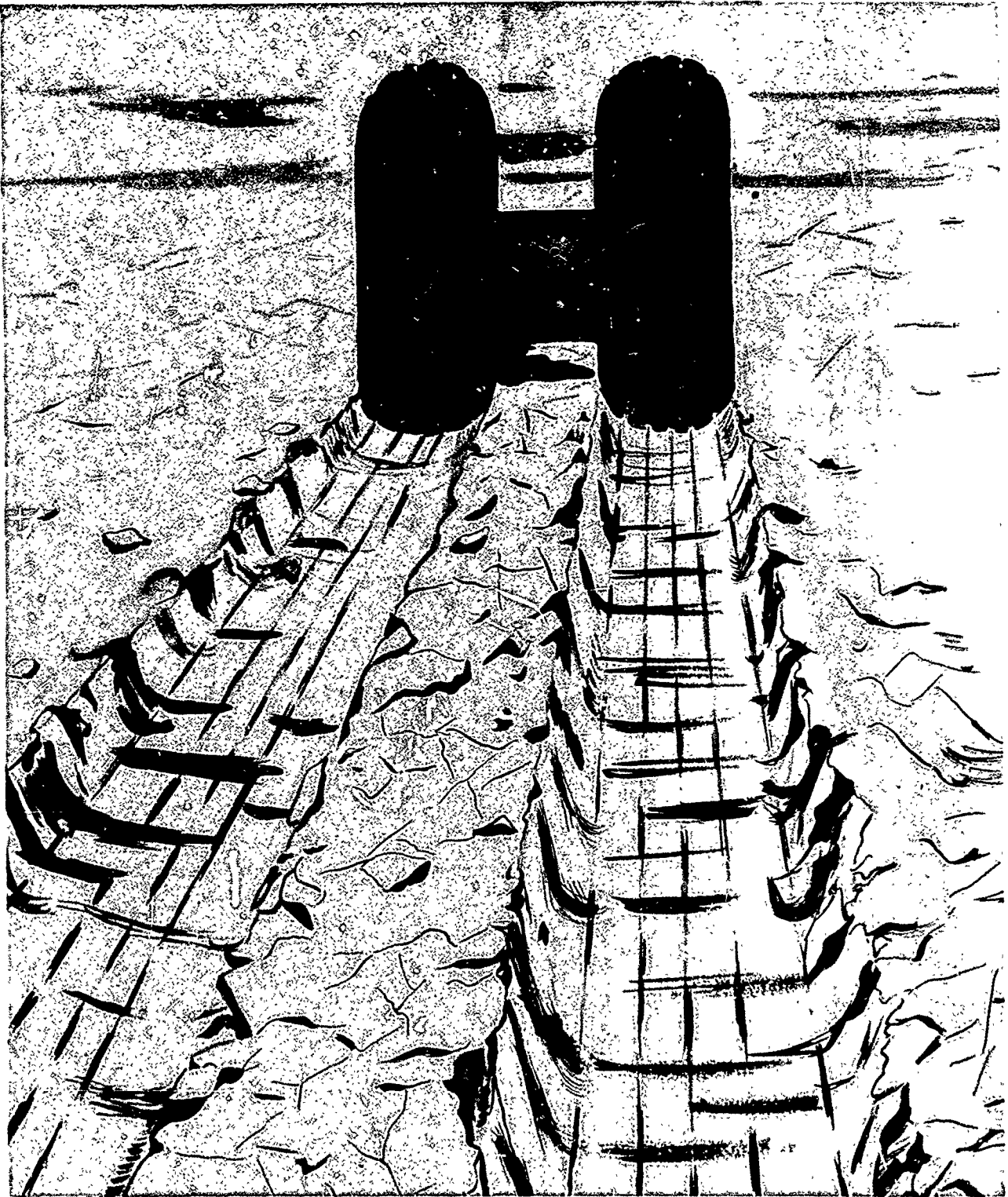


Figure 1 Aircraft Tire Sinkage

SECTION II
IDENTIFICATION OF VARIABLES

1. Literature Review

In studies conducted to date on mobility and flotation, numerous variables have been postulated as influencing aircraft response and landing gear - soil interaction for aircraft operating on semi- and unprepared soil runways. Existing literature discusses these variables in terms of traction wheels and transport wheels. Since the behavior of an aircraft tire is essentially that of a transport wheel, only those variables associated with the transport wheel will be treated. Freitag (1) in a comprehensive review of available mobility data, included tire width, tire diameter, tire inflation pressure, and the cone index (soil parameter) as constituting the primary variables related to drawbar pull (drag) in single wheels. Nuttal (2) included the additional variables of load, tire deflection, vehicle speed, soil viscosity, soil cohesion, and soil friction in analyzing drag and sinkage of wheels. Other researchers (3, 4, 5) considered essentially the same array of variables in analyzing mobility.

2. Analysis of variables

The numerous variables associated with the landing gear - soil interaction all to some extent influence the mechanisms of response in dynamic load situations. Looking first at the characteristics of soil (ground) and the landing gear tires, Table I gives a list of the significant variables commonly specified, without at this stage involving any interaction phenomena.

TABLE I
Significant Variables: Soil, Landing Gear Tires

<u>Soil</u>		<u>Landing Gear Tires</u>
<u>Elastic</u>	<u>Failure</u>	
G = Shear Modulus μ = Poisson's Ratio ρ = Mass Density	c = Cohesion ϕ = Friction	Contact Area and Geometry* Inflation Pressure Tire Ply Rating Tire Stiffness Tire Deflection Contact Stress Distribution Diameter and Width of Tire Number of Tires Tire Spacing and Configuration Tread Pattern

Coefficient of Friction: Tire-Ground

* Other landing gear variables associated with landing gear - soil interaction not considered in this study include: landing gear stiffness, braking system, antiskid and steering system effects.

Upon introducing dynamic loading conditions and relating the problem to interaction phenomena, the number of variables increases significantly. Figure 2 provides a systematic overall look at the interaction problem. Analysis of existing literature indicates that the suitability of soil airstrips for aircraft operations is directly related to vertical sinkage of the aircraft wheel, ground drag, and roughness of the runway surface. On this basis, the interaction problem can be defined in terms of:

- (1) Loads
- (2) Soil Characteristics
- (3) Vehicle Characteristics
- (4) Surface Characteristics

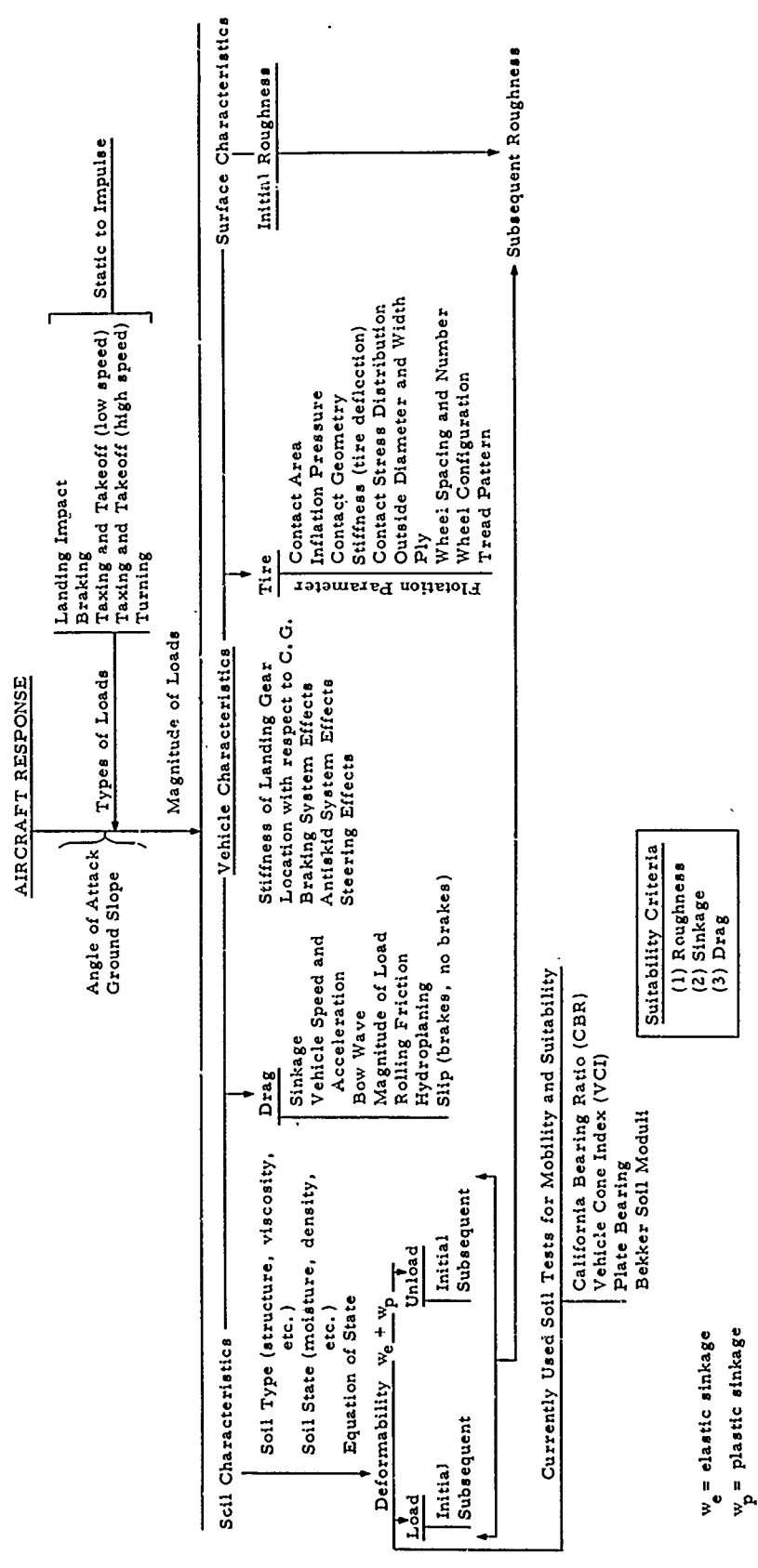
The most important property of soil is its deformability characteristics in loading and unloading. Equations of state relating load to sinkage have been developed by a number of researchers in mobility (1, 3, 4).

Directly related to the loading and unloading characteristics of soil is the residual permanent deformation for each wheel passage. This permanent deformation, when combined with the initial runway roughness, determines the ground roughness for subsequent aircraft operations.

In addition to the deformability of soil, the tire characteristics also influence the resultant sinkage of an aircraft wheel under fixed loading conditions. The numerous variables associated with tire characteristics, as indicated in Figure 2, can be thought of in terms of a flotation parameter, F , related to sinkage. This flotation parameter could then be used to compare landing gears (all other conditions being constant except the tire characteristics) to provide a rational means for selecting the higher flotation gear system.

The third significant quantity in defining suitability of a landing gear for operation at a site is ground drag on the aircraft wheel due to the wheel - ground interaction. While drag is helpful in a landing operation, large drag magnitudes in takeoff operations leads to excessive runway length requirements. The possibility also exists of immobilization of the aircraft. As indicated in Figure 2, ground drag is influenced by load, soil, and vehicle characteristics. Subsequent analysis has indicated that over a significant portion of the aircraft horizontal velocity range the dominant parameter in determining drag is aircraft wheel sinkage.

SUITABILITY = f [surface deformation (sinkage), roughness, drag]



Suitability Criteria

(1) Roughness
(2) Sinkage
(3) Drag

w_e = elastic sinkage
 w_p = plastic sinkage

Figure 2 Variables in Landing Gear-Unprepared Runway Problem

The large number of variables listed in Figure 2 can be interpreted in terms of:

- (1) loads
- (2) deformability of soil
- (3) flotation parameter and flotation index
- (4) initial roughness

if sinkage, drag, and roughness are utilized as the significant quantities in defining the suitability of an unprepared site for aircraft operations.

SECTION III
DRAG-SINKAGE ANALYSIS

1. Drag Analysis

The drag forces exerted by the deformed ground on the aircraft wheel are an important consideration in relation to aircraft thrust for determining the takeoff capability and runway length for aircraft operations on soil surfaces. Figure 3 shows the pneumatic wheel - ground interaction phenomena resulting in drag forces being exerted on the wheel. In this report, sinkage, Z , is defined as the instantaneous displacement of the ground beneath the tire from its equilibrium position (see Figure 3). Depending upon the inflation pressure, a pneumatic tire may act as either a rigid wheel or a nonrigid (flexible) wheel on soft ground. The numerous mobility and flotation studies (1, 2, 3, 6) conducted in the past decade have provided considerable empirical and semi-theoretical information on the drag characteristics of rigid and flexible wheels on rigid surfaces. Considerably less information is available for wheel drag on soft surfaces.

2. Drag Variables

The pertinent variables affecting drag as shown in Figure 2 are summarized in Table II.

TABLE II
Drag Variables

Quantity	Drag	Load	Slip	Cohesion	Friction Angle	Poisson's Ratio	
Symbol	R	P	S	c	ϕ	μ	
Units	F	F	-	FL^{-2}	-	-	
	Shear Modulus	Mass Density		Soil Viscosity		Impingement Drag Coefficient	
	G	ρ		η		C_{DI}	
	FL^{-2}	$FL^{-4}T^2$		$FL^{-2}T$		-	
	Velocity	Acceleration		Contact Area	Tire Width	Tire Diameter	Coefficient of Friction
	V	g		A	b	D	λ
	LT^{-1}	LT^{-2}		L^2	L	L	-

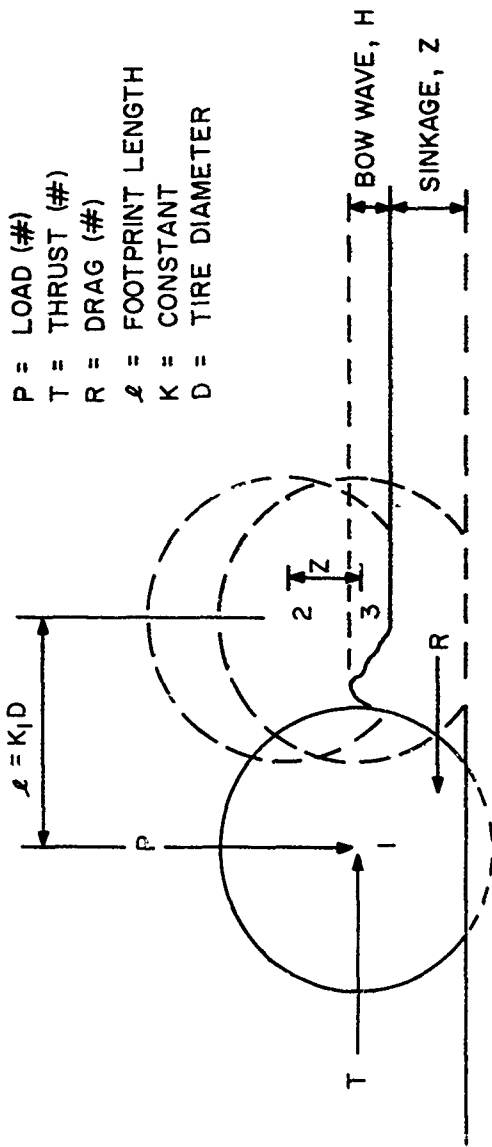


Figure 3 Wheel-Ground Interaction

The effect of horizontal aircraft velocity on drag is indicated in Figure 4 which shows the experimentally measured trend of the drag ratio (Drag/Vertical Wheel Load) with horizontal velocity (5). Reference to Figure 4 indicates at least three distinct zones of drag ratio response. At low speeds (less than 5 knots), the drag ratio changes considerably with velocity due to the viscous effects of the soil as related to tire sinkage. From 5 knots to approximately 40 to 50 knots, the drag ratio is relatively constant, indicating that the rate of loading effects in the soil are no longer significant. In the third region (greater than approximately 40 to 50 knots), the drag ratio increases rapidly with increasing velocity and then diminishes apparently due to the combined effects of soil inertia drag and hydroplaning effects. It should be recognized that even though the drag ratio increases rapidly in the third region, the resultant drag force (which is the critical factor in determining runway length) very likely remains less than the drag in region two, due to the large lift effects at the higher horizontal velocities and consequent reduction in vertical wheel loads.

Assuming that immobility under static loads is not a problem, the most critical drag effects occur in region two and three. Other than limited experimental data indicating the variation of the drag ratio with horizontal velocity, little information is available for understanding the interrelationship between drag, sinkage, high velocity, and soil inertia. On the assumption that a tire traversing soil at high velocities responds the same as a tire traversing slush at high velocities, Boeing (5) utilized the drag equations developed for slush conditions to interpret high velocity soil drag in the form:

$$D' = K C_{DI} Z V^2 \quad (1)$$

where D' = additional drag due to soil inertia effects
 K = constant related to soil density (ρ) and
 tire width (b) = $1/2\rho b$
 C_{DI} = impingement drag coefficient related to soil
 Z = instantaneous sinkage
 V = horizontal velocity

The drag magnitude defined by Equation 1 must be added to the drag developed in region two to determine the total drag acting on the tire in region three. Very little experimental data or theoretical justification is available for proving or disproving the validity of Equation 1. Also, the soil impingement drag coefficient is not known for varying soil types. More recently, Lockheed (6) has begun high speed drag ratio tests which should provide additional information for establishing a relationship between drag, sinkage, and soil inertia at high velocities.

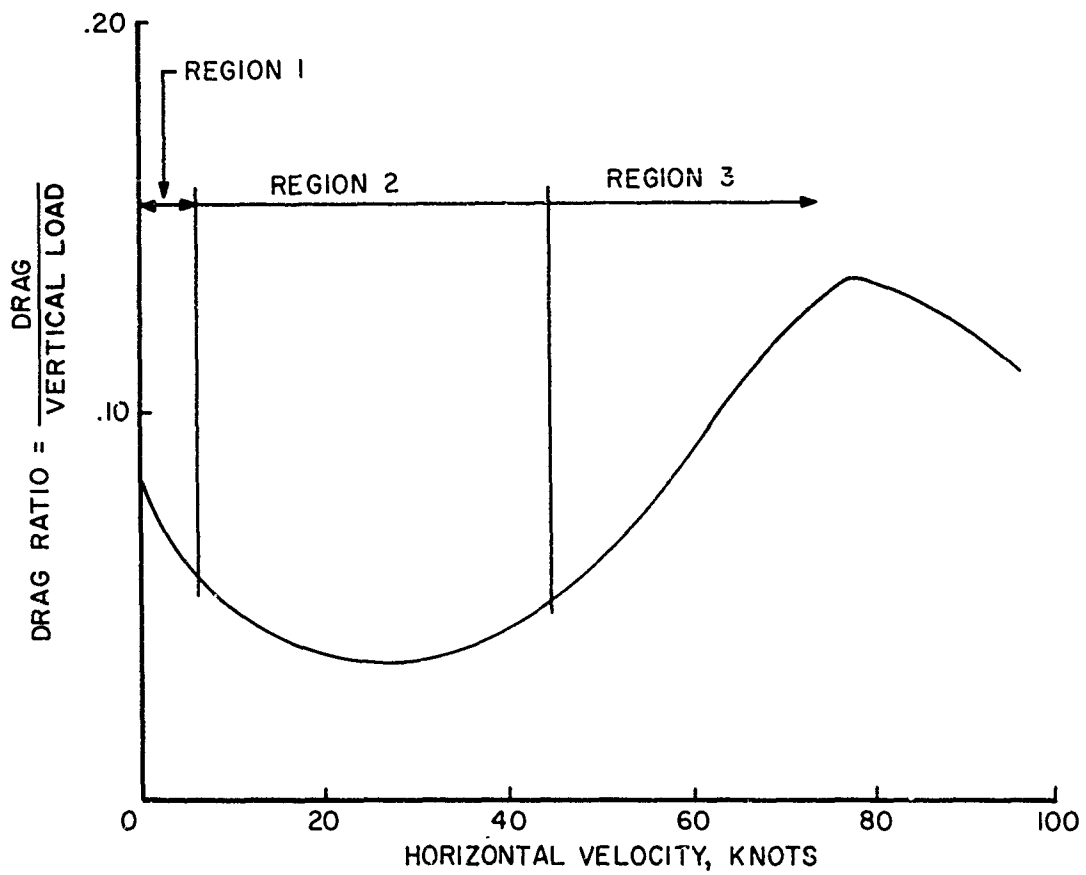


Figure 4 Drag Ratio vs Horizontal Velocity on Soil

3. Drag-Sinkage, Single Wheel

In region two, experimental evidence exists which indicates that the effects of velocity, slip, viscosity, soil density, and soil inertia have only a small influence on drag characteristics. The rolling resistance at zero sinkage is also small in comparison to the total drag at sinkages normally encountered in soil.

A dimensional drag analysis of the remaining variables in Table II could take the form:

$$R/P = f\left(\frac{P}{cD^2}, \varphi, \frac{A}{bD}, \mu, \frac{G}{c}\right) \quad (2)$$

Additionally, if it is recognized that the primary factors related to sinkage, Z , are the load (P), geometry factors (b, A), and the soil properties (μ, G, c, φ), then a simplified drag ratio relationship of the form given in Equation 3 is obtained.

$$R/P = f(Z/D) \quad (3)$$

The inclusion of the wheel diameter, D , in the drag ratio equation is based on simple work-energy relationships which provide an approximation to drag analysis for region two velocity rolling pneumatic tires. Reference to Figure 3 indicates that the work required to increase the potential energy of the wheel as it moves from position 1 to position 2 is $R \cdot \ell$ where ℓ is related to the diameter, D , and consequently can be written as: $R = K_1 D$. The soil, however, undergoes a deformation, the sinkage Z (see position 3) which results in the work quantity (or energy loss): $K_2 PZ$. Neglecting any other forms of energy, the work-energy equation becomes

$$RK_1 D = K_2 PZ \quad (4)$$

or

$$R/P = f(Z/D) \quad (5)$$

Such a simplified drag ratio relationship can also be developed by reference to existing mobility literature. Bekker (3) has examined the relationship among load, tire diameter, and drag for pneumatic tires on soil using a load-sinkage relationship of the form

$$p = \left(\frac{k_c}{b} + k_\varphi\right) Z^n \quad (6)$$

where p = contact stress
 k_c, k_φ = soil deformation moduli
 n = exponent of sinkage
 b = smallest dimension of contact area

For the case of $n = 1$, and neglecting the rolling resistance at zero sinkage, the drag equation as given by Bekker (3) becomes

$$R = \frac{b}{2} \frac{(p_i + p_c)^2}{(k_c + bk_\varphi)} \quad (7)$$

where

p_i = inflation pressure

p_c = carcass pressure

The vertical equilibrium force on the tire is approximately given by

$$P = b\ell_1(p_i + p_c) \quad (8)$$

where

ℓ_1 = contact length between tire and ground

P = total load on tire

Combining equations (6) and (7) and noting that

$$Z = \frac{b(p_i + p_c)}{(k_c + bk_\varphi)} \quad (9)$$

leads to

$$R/P = \frac{Z}{2\ell_1} \quad (10)$$

Recognizing that ℓ_1 is related to the diameter of the tire, D , (i. e., for constant tire deflection, ℓ_1 varies with D) then Equation 10 can be written as

$$R/P = f(Z/D) \quad (11)$$

While it might be reasoned that ℓ_1 is related to both the tire diameter and the tire deflection, d , the effects of the tire deflection are inherent in the sinkage, Z , which includes the inflation pressure, p_i . The form of the drag ratio relationship as given in Equation 11 can also be established from a mobility analysis by Nuttal (2).

On the basis of the above analysis and a review of the literature, an investigation was made of the relationship between drag and sinkage based on existing experimental evidence. While numerous drag studies have been conducted, the measurement of sinkage in many cases was not taken. Figure 5 presents the drag ratio (R/P) versus sinkage ratio (Z/D) based on data from four sources (1, 2, 3, 7). The plotted data includes the full range of soil type (sand to clay) and tire diameters from approximately 30" to 70" which encompasses the range of tire sizes for heavier military aircraft. In reference to Figure 5, it is clearly evident that there is an increasing trend of the drag ratio with increasing sinkage ratio for Z/D varying from 0 to 0.10.

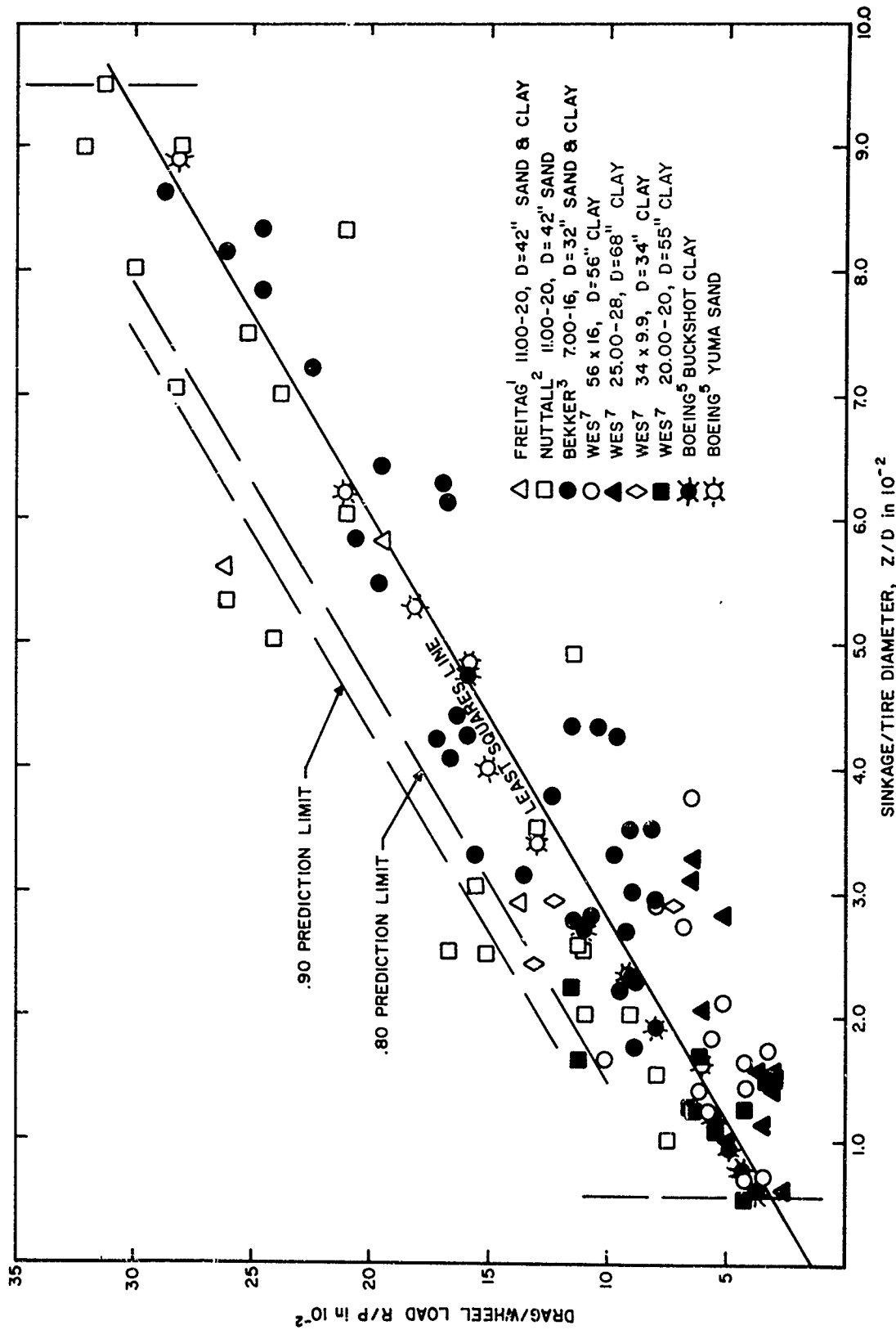


Figure 5 Drag Ratio-Sinkage Ratio, Single Wheel on Soil

Little interest is given to the relationship beyond a Z/D of 0.10, since for a 30" diameter tire, the sinkage would be in excess of 3" which is presently the instantaneous sinkage normally specified as a failure sinkage for military aircraft (9).

It is also evident from analysis of Figure 5 that there is a considerable amount of scatter in the data. This scatter may arise from several causes. The full range of soil type is included in the analysis. As additional drag-sinkage data becomes available, the effect of soil type may be more clearly recognized. In some instances the data sources do not specify whether the definition of sinkage does or does not include the bow wave, H (see Figure 3). Sinkage as utilized in this report does not include the bow wave (H). Additionally, soil viscosity effects may be present to some extent for those test data obtained at the lower velocities. Also it is possible that the sinkage quantity, Z, may not adequately reflect the variables b (tire width), and d (tire deflection).

In general, however, Figure 5 suggests that the most significant variables as related to drag are the load (P), sinkage (Z), and tire diameter (D). Consequently, a least squares linear and a least squares parabola were fitted to the data with the sinkage ratio as the independent variable and the drag ratio as the dependent variable. Analysis of the results indicated that the quadratic term was not a significant contributant to the drag relationship in the range of Z/D considered and therefore based on the experimental data, the drag ratio - sinkage ratio relationship is given by

$$R/P = 0.015 + 3.09 (Z/D) \quad (12)$$

The positive R/P intercept at zero sinkage would be expected since some rolling resistance (friction) is present at zero sinkage.

Of additional interest is the determination of the upper bound drag magnitudes likely to be encountered by an aircraft on an unprepared landing site when the characteristics of the aircraft and approximate sinkage values (based on soil type and conditions) are known. For this purpose 80% and 90% probability lines were established and are shown in Figure 5. This upper bound drag, when related to aircraft thrust capability, should be helpful in determining runway lengths and possible immobility conditions for aircraft operating on semi- and unprepared land sites.

Subsequent to the least squares analysis used to establish Equation 12, additional drag data became available from tests reported by Boeing (5). This additional data is shown in Figure 5 and tends to verify the established relationship.

4. Drag-Sinkage, Twin, Tandem Wheels

Very little information (theoretical or experimental) is available concerning multiple wheel effects as related to drag forces on aircraft wheels. Two types of multiple wheel configurations are of interest: dual

and tandem. Dual wheels at very large spacings tend to act as single isolated wheels. The drag relationship for closely spaced wheels is not known. Similarly, the drag relationship for tandem wheels where one wheel follows in the path of the first wheel has not been adequately determined.

In analyzing multiple wheel effects on drag based on existing experimental data (1965), Freitag (1) concluded that in frictional soils existing data indicated that each wheel in a dual pair performs at the same level as an isolated single wheel for all dual wheel spacings. Analysis of dual wheel effects in frictionless soils permitted no conclusions due to insufficient and inconsistent data. Even the conclusions drawn from studies in frictional soils are questionable, due to the limited test data and the fact that the test data covered only two tires with a range in wheel diameter from 24" to 40", while dual tire spacing ranged from 8" to 16".

A limited amount of additional test data involving drag measurements for multiple wheels is available from a recent WES (7, 9) flotation investigation on clay soil. Twin wheel and multiple wheel (twin-twin or twin-tandem) configuration tests were conducted. An indication then of multiple wheel effects can be gained by analyzing the drag sinkage data from only the WES study. For comparative purposes a linear least squares fit of the WES single wheel data yields the equation (see Figure 6)

$$R/P = 0.030 + 1.65 (Z/D) \quad (13)$$

Due to the limited amount of twin wheel test data, all the twin wheel drag-sinkage data has been plotted in Figure 7 on the basis of taking the total drag and dividing by the total of the wheel loads (converting R/P to a single wheel basis). The twin wheel spacing ranged from 25" to 60". A linear least squares analysis of this test data yields

$$R/P = 0.030 + 1.45 (Z/D) \quad (14)$$

There is no apparent trend in the larger spaced wheels data of lying above the linear least squares line as would be expected if the wheels tended to act as single isolated wheels at larger spacings. Comparison of Equations 13 and 14 (single wheel to twin wheel respectively) indicates that while there is some effect of wheel spacing on the drag ratio-sinkage ratio relationship (less than 15% in the range considered), it is not a pronounced effect. Since most conventional aircraft tires for cargo aircraft cannot be spaced closer than about 20 inches, it appears that each wheel in a twin wheel configuration tends to act as a single isolated wheel in frictionless soils in determining drag characteristics.

Multiple wheel (three or more wheels in both tandem and dual configurations) drag-sinkage data taken from the WES tests is shown in Figure 8. A linear least squares analysis of this data gives

$$R/P = 0.020 + 1.26 (Z/D) \quad (15)$$

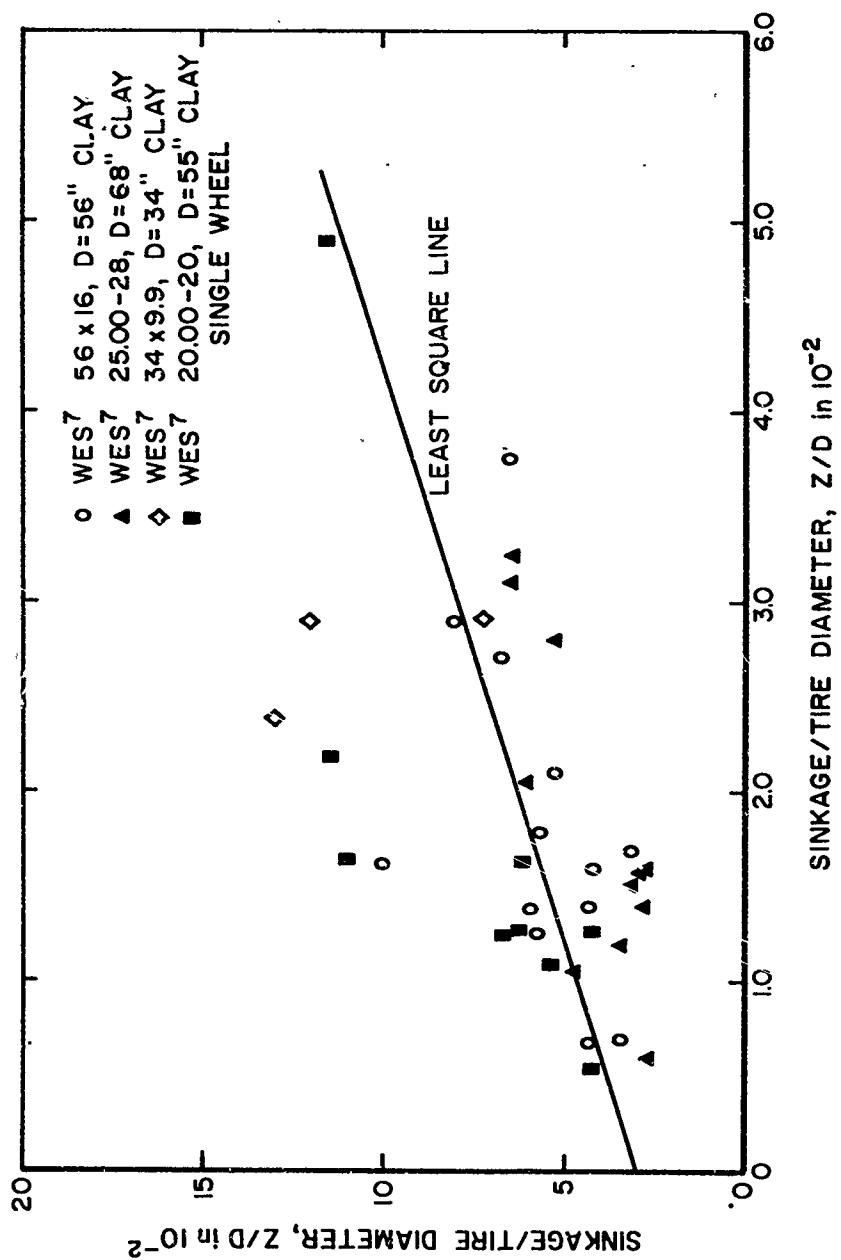


Figure 6 Drag Ratio-Sinkage Ratio, Single Wheel WES Data on Soil

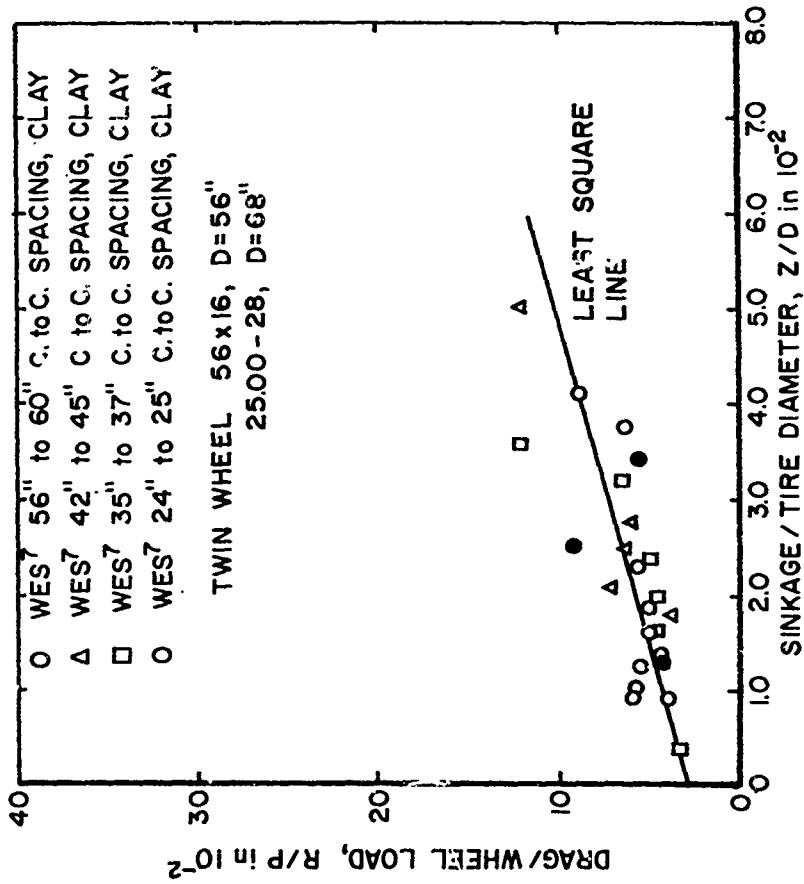


Figure 7 Drag Ratio-Sinkage Ratio, Twin Wheel WES Data on Soil

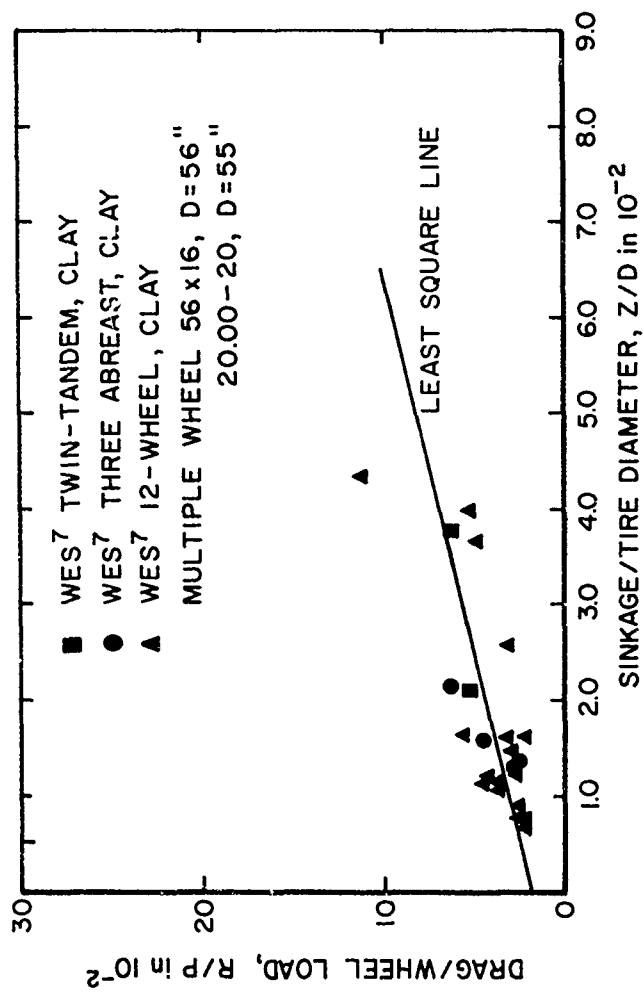


Figure 8 Drag Ratio-Sinkage Ratio, Multiple Wheel WES Data on Soil

There is a considerable difference between Equations 15 (multiple wheel) and Equation 13 (single wheel). This difference is due to tandem effects; that is, wheels following in the same path as forward wheels. Since the lead tire causes ground deflection (with subsequent changes in soil deformability properties) subsequent to the follow-on tire, the tandem tire will undergo less sinkage and consequently less drag.

Based on the limited data presented in Figures 6, 7, and 8, it is difficult to conclude an exact drag-sinkage relationship in frictionless soils for twin and tandem wheel configurations. It would appear, however, that for normal tire spacings, dual wheels tend to act as single isolated wheels in determining drag, whereas a significant reduction in drag (over that determined by considering the wheels as single isolated wheels) can be expected for tandem wheel configurations in frictionless soils.

All of the data used in developing Figures 5, 6, 7, and 8 and the resulting analysis equations are summarized in Appendix I.

5. Summary

Based on the above analysis and evaluation of existing experimental drag data, the critical parameter in determining drag on an aircraft wheel in the Region two velocity range is sinkage of the tire into the soil. If an estimate can be made of the anticipated sinkage, then the total drag can be determined within suitable limits for developing required runway lengths as related to specific aircrafts. As additional drag data becomes available, the drag ratio-sinkage ratio as defined in Figure 5 and Equation 12 can be suitably modified to reflect this additional drag information.

Analysis of aircraft drag ratio response at high velocities (Region three) has not been adequately defined either theoretically or experimentally to permit reliable estimates of drag magnitude. If the high velocity drag relationship as developed by Boeing (5) is utilized, then the drag ratio defining aircraft response in Region three can be treated as the sum of the drag defined by Region two plus the drag determined from Equation 1.

SECTION IV

SINKAGE PREDICTION EQUATIONS

I. General

Since vertical sinkage of the aircraft tire is the dominant factor in determining drag on the wheel in the region two velocity range, and based on the work of Boeing (5) forms the basis for which inertia drag effects must be added for defining drag in the region three velocity range, it is important to analyze the currently used sinkage prediction equations for the reliability and accuracy of sinkage prediction as related to the loading, landing gear, and soil variables. Additionally the sinkage affects aircraft capability to operate from a site due to resulting permanent deformation and roughness effects, and thus forms the basis of flotation analysis.

Numerous experimental and analytical efforts have been undertaken to develop load-sinkage equations which adequately interpret soil properties as related to soil deformation characteristics under loading. Defining soil load-sinkage behavior is an extremely complex problem due to the inherent nonlinear and inelastic behavior of soil. Under low stress loadings, the soil response is approximately elastic. At higher stress levels, which is common to problems in flotation and mobility, the contact stresses are far in excess of any elastic limit for soil. For aircraft wheels moving over soft soils, the complex soil response involves elastic, viscous (time dependent), and plastic deformations.

2. Currently Used Sinkage Equations

Initial efforts at developing load-sinkage equations involved power functions of the sinkage term, Z . The most widely used equation in this form was developed by Bekker (10) as

$$p = \left(\frac{k_c}{b} + k_\phi \right) Z^n \quad (16)$$

where

p = contact stress, psi

k_c, k_ϕ = soil deformation moduli related to friction and cohesion of soil

n = exponent of sinkage

b = smallest dimension of contact area, in.

Z = vertical sinkage, in.

Equation 16 utilizes two soil parameters to account for the frictional and cohesive contributions to soil strength. The Bekker developed load-sinkage

equation is used primarily by the Land Locomotion Laboratory in their studies of both tire and track mobility over soil terrain. Widespread use of Equation 16 has not developed due to the dimensional inconsistency in Z being a power function, and the lack of a consistent trend in k_c and k_ϕ with soil type (negative values of the soil deformation moduli have been reported in some instances).

WES(5) has also developed a load-sinkage relationship specifically for pneumatic tires which is defined in terms of a clay mobility number (CMN) and a sand mobility number (SMN). These mobility numbers as defined in Equations 17 and 18 are developed from cone index readings which are a measure of the resistance of the soil to penetration by a cone tipped rod.

$$\text{Clay Mobility Number (CMN)} = \frac{(CI)bD}{P} \left(\frac{\delta_t}{h_t} \right)^{1/2} \quad (17)$$

$$\text{Sand Mobility Number (SMN)} = \frac{(G)(bD)^{3/2}}{P} \left(\frac{\delta_t}{h_t} \right) \quad (18)$$

where

CI = average cone index over first six inches, psi

G = slope of cone index versus depth averaged over a depth equal to the tire width, psi per in.

b = tire width

δ_t = tire deflection, in.

h_t = tire section height, in.

Approximations to the mean sinkage ratio-mobility number (5) yields

$$\frac{Z}{D} = 0.003 + (\text{CMN})^{-2.6} \text{ for } 3 \leq \text{CMN} \leq 10 \quad (19)$$

$$\frac{Z}{D} = 0.003 + (\text{SMN})^{-1.5} \text{ for } 5 \leq \text{SMN} \leq 40 \quad (20)$$

Equations 19 and 20 which define sinkage in the extreme soil types (sand and clay) were developed by a dimensional analysis of the experimental data taken from pneumatic tire tests on only two soils, Yuma sand and Buckshot clay. Consequently the extension of Equation 19 and 20 to other soils and conditions is questionable at the present time.

An alternate approach to defining a load-sinkage relationship has been developed by Assur (11) who considered three possible modes of soil response as given by:

$$p = K_s Z \left(1 - \left(\frac{K_s \cdot Z}{p_m} \right)^2 + 2 \left(\frac{K_s \cdot Z}{p_m} \right)^4 \dots \right) \quad (\text{fluidization}) \quad (21)$$

$$p = \frac{K_s \cdot Z}{1 - Z^2/Z_m^2} \quad (\text{compaction}) \quad (22)$$

$$p = \frac{K_s \cdot Z}{1 + Z^2/Z_m^2} \quad (\text{collapse}) \quad (23)$$

where

K_s = coefficient of subgrade reaction, psi per in.

p_m = maximum bearing strength, psi

Z_m = sinkage at maximum bearing strength, in.

While these load-sinkage equations can be used to approximate almost any observed load-sinkage response of soil (through curve fitting techniques), it is not always evident in attempting to predict sinkages, the value of the maximum bearing strength (p_m) and the sinkage at the maximum bearing strength (Z_m). Also these equations are not related to any fundamental soil property which hinders their utility of use.

More recently Boeing (5) developed a load-sinkage equation analogous in form to the equation of Bekker. The nonlinear relationship between load and sinkage is accounted for in Boeing's equation by use of a nonlinear instantaneous dynamic soil spring rate (k_d) as shown in Equation 24.

$$Z = \frac{P}{A k_d} \quad (24)$$

where

$k_d = k_s D_y^\Psi$ = instantaneous dynamic soil spring rate,
psi per in.

and

k_s = static soil spring rate, psi per in.

D_y = dynamic factor related to duration of loading (taken as
unity for frictional soils)

Ψ = attenuation factor which varies with sinkage

A = contact area, in.²

By letting $n = 1$ in Equation 16, and defining the dynamic soil spring rate as

$$k_d = \left(\frac{k_c}{b} + k_\phi \right)$$

it is evident that Equations 16 and 24 are similar in form.

Because of the broad range and number of variables selected in developing these sinkage relations and due to the fact that the expressions for sinkage vary from analytical with little experimental justification to strictly empirical formulations, it is difficult to define which of these sinkage prediction equations is most suitable and accurate for predicting sinkages of aircraft tires into soil. If a suitable correlation existed between the numerous soil parameters, a more comprehensive and meaningful study of flotation could be made utilizing experimental data from many sources. No valid relationship has been established at the present time between the soil parameters defined in Equations 16, 17, 18, 21, 22, 23 and 24.

3. Limited Correlation of Sinkage Prediction Equations

An extension of the recent work by Janosi (12) when combined with experimentally established relationships between the California Bearing Ratio (CBR) and the cone index (CI) permits a limited correlation between Bekker's moduli of soil deformation and WES's cone index for sands and clays. Based on the definition of the static soil spring rate, this correlation can also be extended to include Boeing's soil parameter, k_s .

The correlation between soil parameters is based on an analysis of the cone penetration test. The cone penetration test as developed by WES (1) consists of measuring the pressure required to force a standard cone tipped rod into soil. The cone index (CI) then is defined as the measured pressure. The equivalence between Bekker's soil parameters and WES's cone index as developed by Janosi (12) is given by

$$CI = 1.625 \left\{ \frac{k_c}{n+1} \left[(Z+1.5)^{n+1} \right] - Z^{n+1} + 0.5175 k_\phi \left[\frac{(Z+1.5)^{n+2}}{(n+1)(n+2)} + \frac{Z^{n+2}}{n+2} - \frac{(Z+1.5)}{n+1} Z^{n+1} \right] \right\} \quad (25)$$

a) Sinkage in Sand

For sands, k_c is zero and experimental evidence indicates that $n=1$ is approximately valid. For these conditions Equation 25 reduces to

$$CI = k_\phi (0.947Z + 0.474) \quad (26)$$

As indicated in Equations 18 and 20, the sand mobility number (SMN) is related to sinkage. The quantity G which is defined as the slope of the cone index versus depth curve averaged over a depth equal to the tire width is used to define the properties of sand. By differentiating Equation 26, the quantity G becomes

$$G = \frac{d(CI)}{dZ} = 0.947 k_{\phi} \quad (27)$$

By definition the cone index is the pressure required to penetrate the cone tipped rod into soil. Boeing's static soil spring rate can then be developed from Equation 26 as

$$k_s = \frac{P}{Z} = \frac{(CI)}{Z} = k_{\phi} \left(0.947 + 0.474 \frac{Z}{Z} \right) \quad (28)$$

or in terms of the parameter G,

$$k_s = G \left(1.0 + \frac{0.5}{Z} \right) \quad (29)$$

Based on these relationships between k_{ϕ} , G, and k_s , and noting that the tire contact area, A, is given by (13)

$$A = fD^2 \quad (30)$$

where

f = coefficient related to the tire type and tire deflection
D = tire diameter, in.

Bekker's sinkage equation can be put in the form

$$\frac{Z}{D} = \frac{0.947P}{GfD^3} \quad (31)$$

where

Z/D = sinkage ratio

Combining Equations 24 and 29 leads to Boeing's sinkage equation in the form

$$\frac{Z}{D} = \frac{P - 0.5 \psi G f D^2}{\psi G f D^3} \quad (32)$$

The appropriate ψ values were developed by Boeing (5). By combining Equations 18 and 20, WES's sinkage equation becomes

$$\frac{Z}{D} = 0.003 + \left[\frac{G(bD)^{3/2}}{P} \left(\frac{\delta_t}{h_t} \right) \right]^{-1.5} \quad (33)$$

In order to compare these sinkage equations, the trend of the sinkage ratio versus increasing load was examined for a 20.00-20 type III tire at

33-1/3% tire deflection (d). The results of this comparison are given in Figure 9 for the common soil parameter, G , taking on values of 5, 10, and 20. The G values of 5 and 20 could approximate a frictional soil in a loose and medium dense condition respectively. The corresponding values of k_s for the Boeing sinkage equation and k_ϕ for the Bekker sinkage equation for each selected G value as developed from Equations 27 and 28 are also indicated in Figure 9. This comparison is not an attempt to study the exactness of the magnitude of sinkage, but rather to examine trends with increasing loads. It is evident however that even though each sinkage equation utilizes the same G value based on the above correlation, that the sinkage ratio varies by up to 100% or more between these sinkage equations under like conditions. Also it is noted that the trend of the sinkage ratio prediction as given by Boeing is such as to intersect the trend of the sinkage ratio prediction as given by the Bekker and WES equation.

One way in which increased flotation (reduced sinkage) can be developed for pneumatic tires is by increasing the tire deflection (decreasing tire inflation pressure). In order to examine the trend of this increased flotation with increasing tire deflection, Equations 31, 32, and 33 were evaluated for a 20.00-20 tire subjected to a 6000 lb_w wheel load on a $G=5$ sand soil. The results of this evaluation are shown in Figure 10. While no system has been developed for rating increased flotation as related to tire and soil variables, it is evident from reference to Figures 10 and 5 that by increasing the tire deflection from 15% to 30%, a decrease in the magnitude of drag forces of between 40% and 50% will occur for the 20.00-20 tire under these conditions.

Increased flotation can also be developed by increasing the width of tires. Figure 11 indicates the variation in sinkage ratio with increasing tire width for a 55 inch diameter tire at 30% tire deflection on a sand soil ($G=5$) as determined from Equations 31, 32, and 33. While the magnitude of the sinkage ratio is quite different as determined from each sinkage equation, reference to Figures 11 and 5 indicates that the effect of varying the tire width from 15" to 25" is to decrease the magnitude of drag by approximately 50% under these conditions.

b) Sinkage in Clay

Correlation of the soil parameters related to clay type soils is not as evident as in the case of sands and must rely to a limited extent on the empirical relationships established by experimental test data as related to the CBR and cone index.

For clay type soils, experimental data indicates a range of n values in Bekker's equation of between 0.15 to 0.40. From Janosi (12) a relationship can be established between the CBR at 0.2 inch penetration and Bekker's soil parameters k_c and k_ϕ using $n=0.25$ as given in Equation 34.

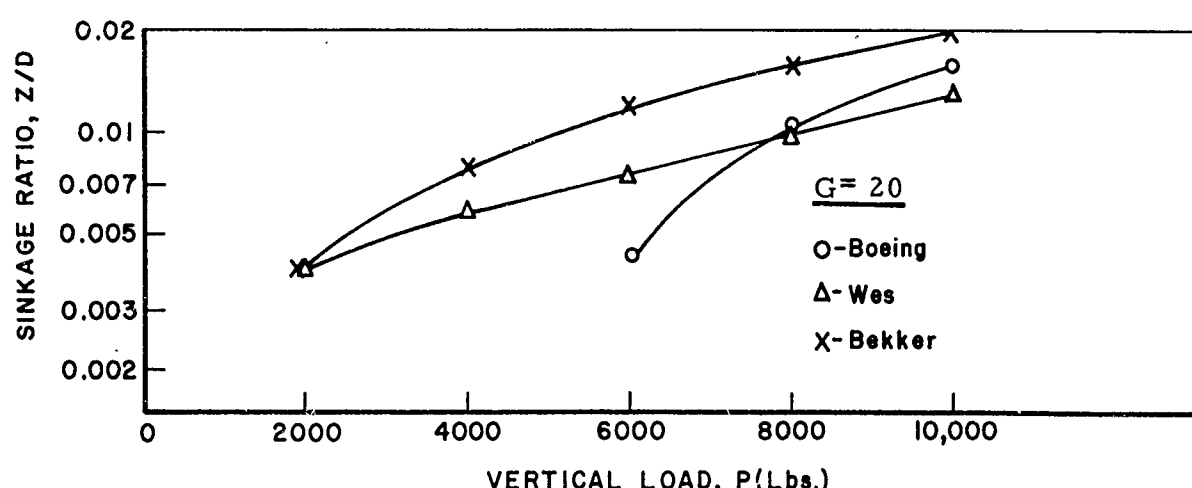
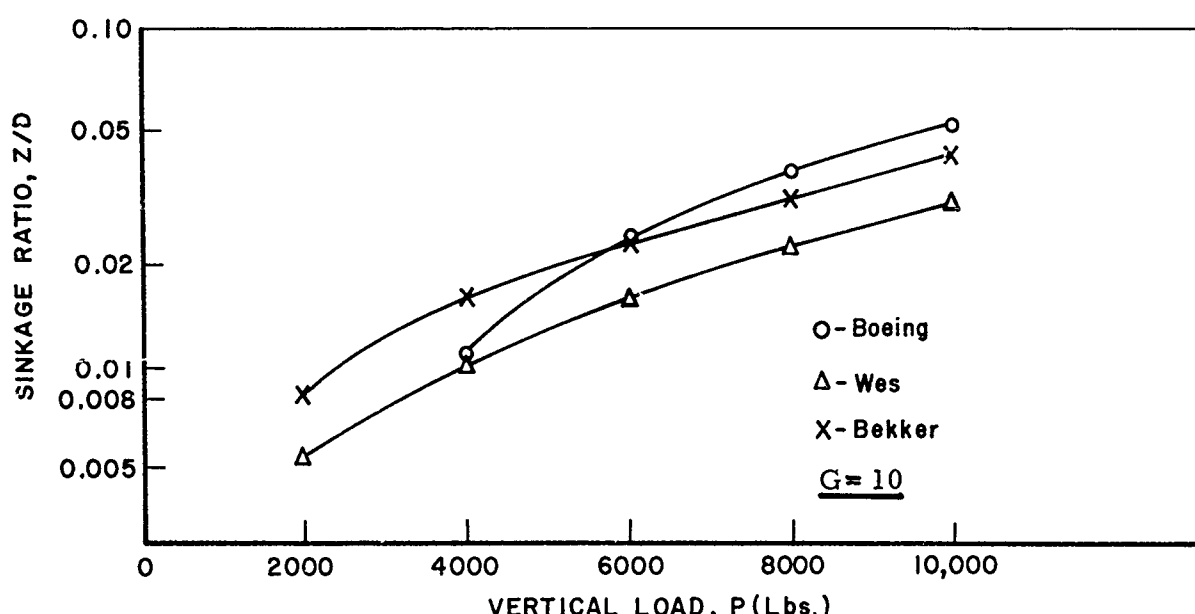
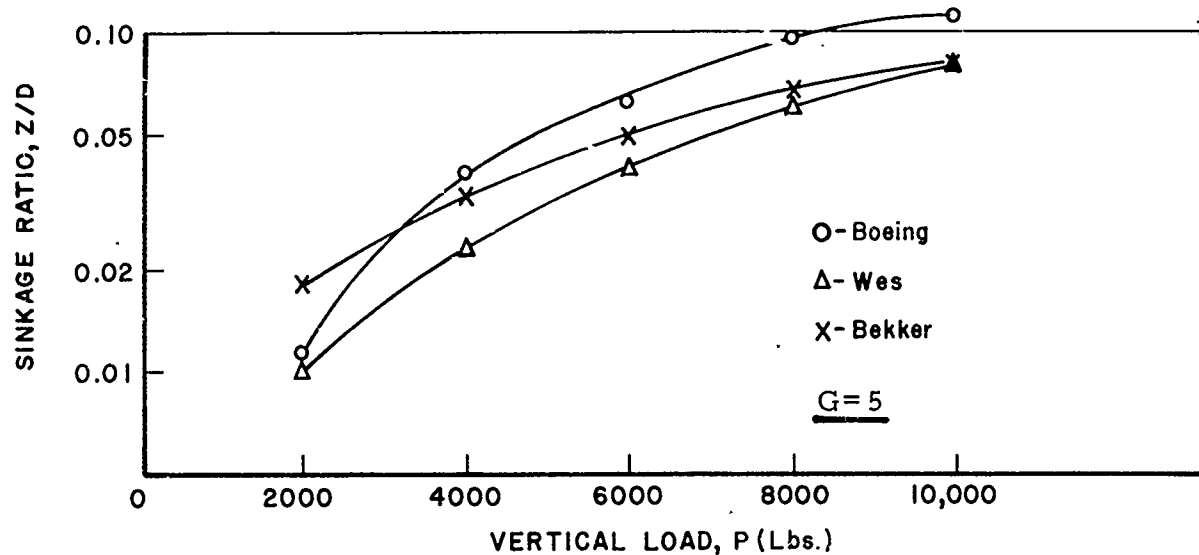


Figure 9 Sinkage Ratio vs Wheel Load, 20.00-20 Tire, $d = 33\frac{1}{3}\%$ on Sand Soil, $G = 5, 10, 20$

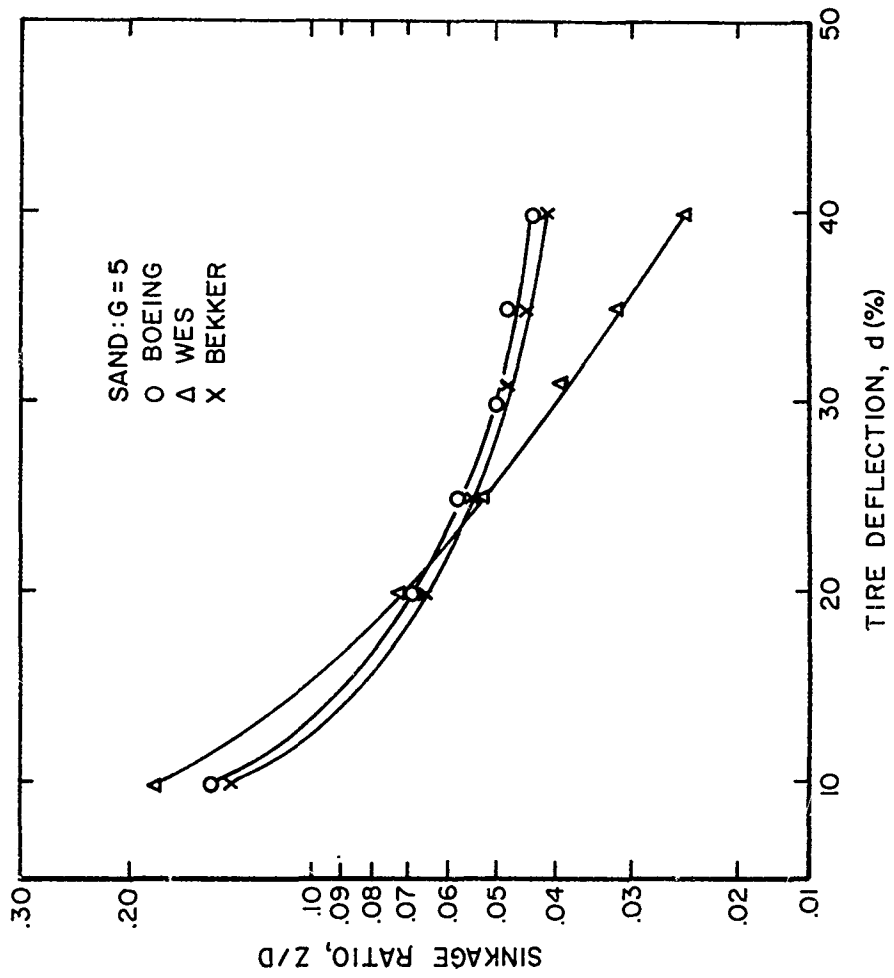


Figure 10 Sinkage Ratio vs Tire Deflection, 20.00-20 Tire,
 P=6000 lbs on Sand Soil

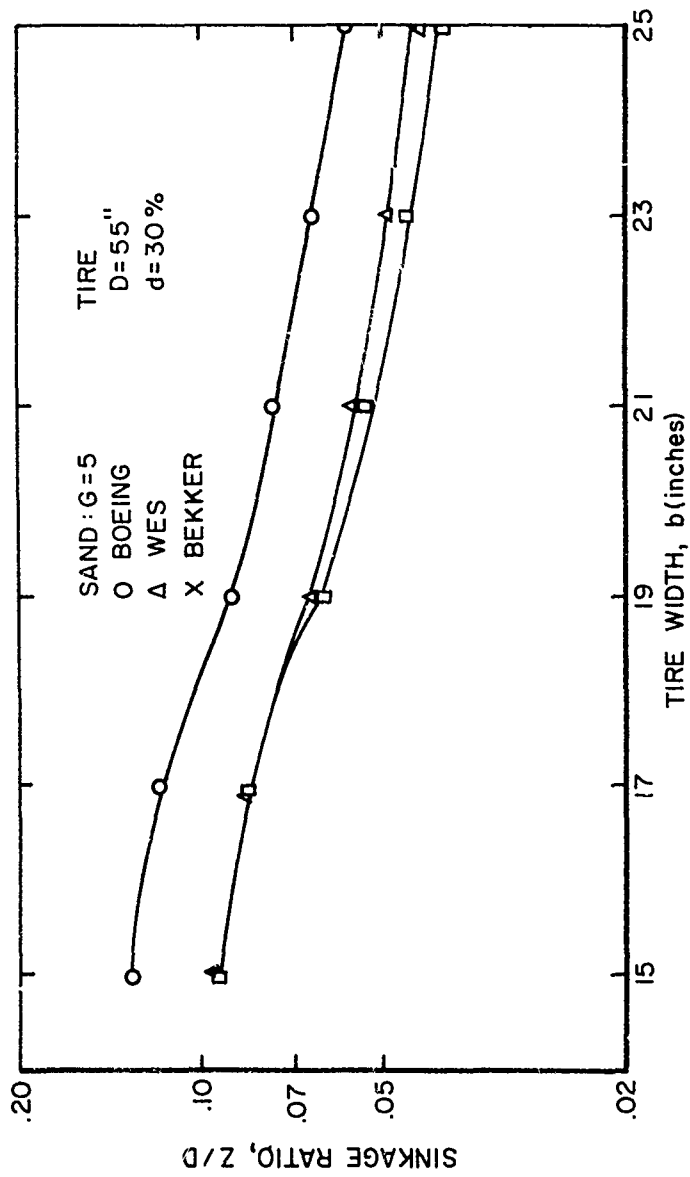


Figure 11 Sinkage Ratio vs Tire Width, 50 inch Diameter Tire, P = 6000 lbs on Sand Soil

$$\text{CBR} = r^2 \left(\frac{k_c}{r} + k_\phi \right) (0.2)^{0.25} \times \frac{100}{4500} \quad (34)$$

where

r = radius of the CBR piston.

For $r = 1.97''$, Equation (34) becomes

$$22.3 \text{ CBR} = 1.02 k_c + k_\phi \quad (35)$$

The results of an extensive correlation between the CBR and the cone index by Scala (14) indicated that for clay type soils, the cone index at 5 inches penetration can be related to the CBR at 0.2 inch penetration through the approximate relationship: $\text{CI} = 50 \text{ CBR}$. Equation 25 becomes then

$$\text{CI} = 50 \text{ CBR} = 1.625 \left\{ \frac{k_c}{n+1} \left[(Z+1.5)^{n+1} - Z^{n+1} \right] + 0.5175 k_\phi \left[\frac{(Z+1.5)^{n+2}}{(n+1)(n+2)} + \frac{Z^{n+2}}{n+2} - \frac{(Z+1.5)Z^{n+1}}{n+1} \right] \right\} \quad (36)$$

which for $n = 0.25$ and $Z = 5''$ gives

$$50 \text{ CBR} = 3.77 k_c + 1.43 k_\phi \quad (37)$$

Equations 35 and 37 can then be used to define the relationship between k_c , k_ϕ , and CBR as

$$k_c = 7.9 \text{ CBR} \quad (38)$$

$$k_\phi = 14.4 \text{ CBR}$$

Utilizing the relationship of Scala ($\text{CI} = 50 \text{ CBR}$) and Equation 38, the Bekker and WES sinkage prediction equations can be put in the form of sinkage ratio equations as related to the common soil parameter, CBR. Bekker's equation becomes

$$\frac{Z}{D} = \frac{P^4 b^4}{f^4 D^9 (\text{CBR})^4 (7.9 + 14.4b)^4} \quad (39)$$

The sinkage prediction equation of WES can be written as

$$\frac{Z}{D} = 0.003 + \left[\frac{50(\text{CBR})bD}{P} \left(\frac{\delta_t}{h_t} \right)^{1/2} \right]^{-2.6} \quad (40)$$

Equations 39 and 40 were evaluated for a 20.00-20 type III tire at 33-1/3% tire deflection for CBR soil values of 2 and 5. The results of this analysis are given in Figure 12. As for sands, there is considerable difference in the magnitude of the sinkage ratios in the clay soil between each of the sinkage prediction equations.

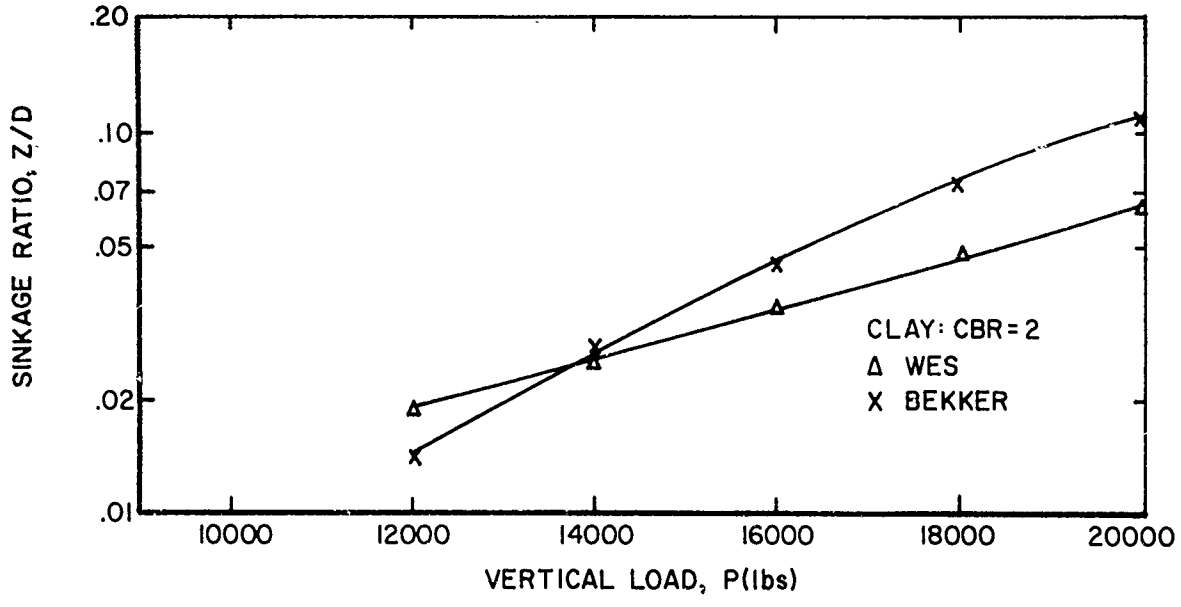
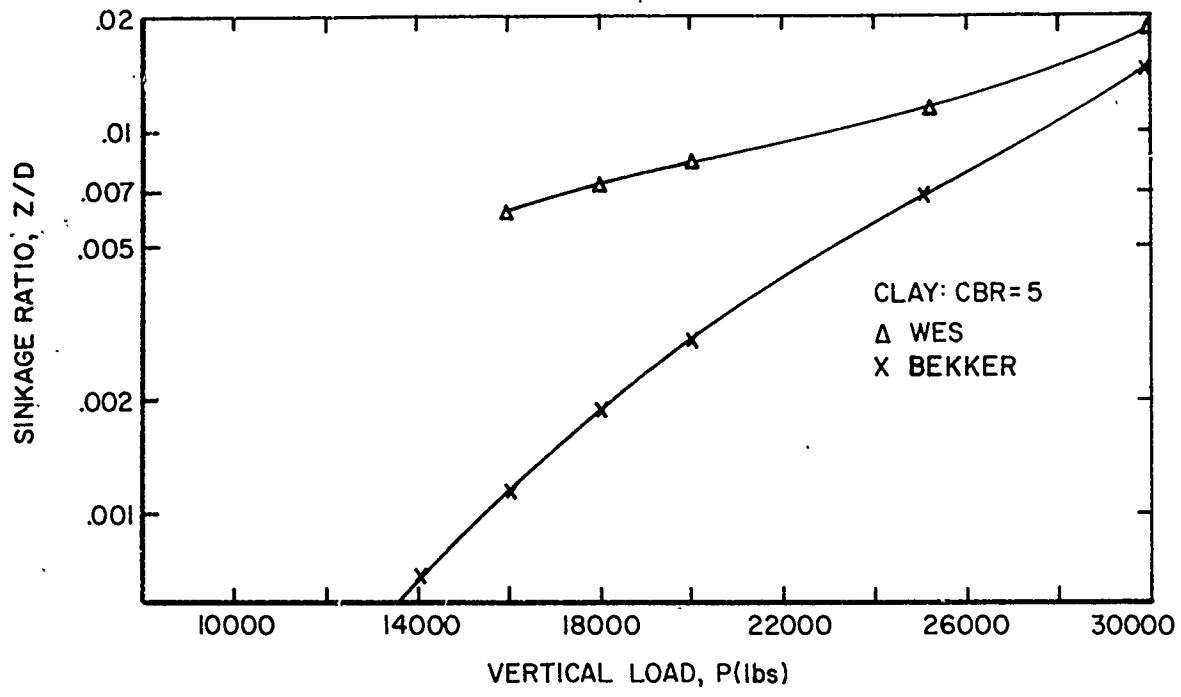


Figure 12 Sinkage Ratio vs Wheel Load, 20,00-20 Tire,
 $d = 33\frac{1}{3}\%$ on Clay Soil, CBR = 2, 5

The effect of increasing tire deflections on the flotation in clay soils is shown in Figure 13 for the same 20.00-20 tire for a CBR of 2 soil and a wheel load of 16,000 lbs. Reference to Figures 5 and 13 show that by increasing the tire deflection from 20% to 30%, an approximate 50% to 60% decrease in the magnitude of drag forces will occur under these particular conditions.

4. Summary

While the above detailed sinkage relationships are not a complete survey of proposed load-sinkage models, they do in general typify past and current efforts in the development of load-sinkage models for soil. At the present time, as indicated in Figures 9 through 13, and as observed from a review of the mobility and flotation literature, the reliability of sinkage prediction using current load-sinkage equations would appear to be in the range of $\pm 50\%$ to $\pm 100\%$. Since, as indicated in Figure 5, the magnitude of drag varies linearly with sinkage (for other factors being constant), similar uncertainties would be associated with estimating drag magnitudes.

In analyzing soil behavior under wheel loads in an effort to develop an analytical expression for load-sinkage based on measured soil properties for flotation analysis, several factors are fundamental to the problem. These factors include:

- a) The analytical expression (model) should be relatively simple to facilitate its use in predicting sinkages as related to soil type.
- b) The resultant model should adequately describe the known response of soil and consequently to varying extents must include: elastic, and plastic behavior, and dynamic effects.
- c) Unloading characteristics must be included to analyze subsequent wheel passage effects.
- d) The resultant model should include soil parameters which are amenable to the existing soil experimental property measurements.

While the above summarized sinkage equations satisfy part of these factors, they are in general tied to an empirical approach including only the surface variables, and are lacking in the inclusion of plastic, dynamic, and subsequent loading effects. Recent studies (15, 16) have shown that plastic behavior of soil is important in analyzing the response of soil to loading. Plastic response is a major factor for contact stress levels normally encountered from pneumatic aircraft tires.

Until sinkage analysis includes the distribution of stress within the soil mass and incorporates plastic and dynamic effects as related to the stress distribution, increased reliability of sinkage estimates will be made only through extensive full scale experimental testing over a wide range of variables. Recent work by Yong (17) has given some insight into the

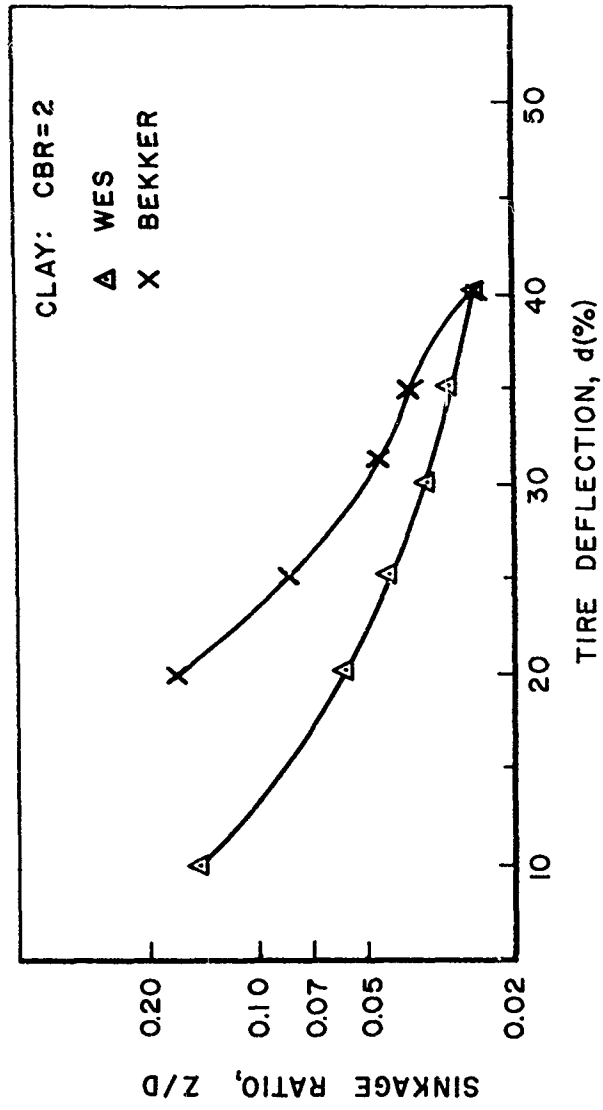


Figure 13 Sinkage Ratio vs Tire Deflection, 20.00-20 Tire,
P = 16,000 lbs on Clay Soil

dynamics of soil response under moving wheel loads. Additionally the use of finite element techniques as applied to the contact element-soil mass problem, wherein the soil response can be treated as an elasto-plastic material, should provide reliable estimates of sinkage as related to the landing gear, load, and soil variables.

SECTION V

FLOTATION PARAMETER

1. General

One of the most critical needs of aircraft landing gear design engineers is the development of a suitable criteria for comparing the anticipated performance (flotation) of landing gear systems on semi- and unprepared runways as an aid in selecting the higher flotation system. The results of the drag and sinkage analysis indicated that sinkage is an extremely important parameter in analyzing performance. A suitable criteria then in developing a flotation parameter (or relative merit index) would be to relate performance to sinkage and to base comparative tire studies and landing gear system studies on sinkage.

The sinkage of an aircraft tire is related to the load, tire characteristics, and soil conditions. Since only a comparison of different tires performance is to be made, the soil conditions will remain constant for comparison purposes which simplifies the problem. Ideally, the determination of the sinkage would be based on total sinkage as developed from an elasto-plastic-dynamic theory which adequately reflects the deformability characteristics of soil. As indicated in Section IV, such a solution is not available at the present time. In order to develop the concept of a flotation parameter based on sinkage and to indicate how comparative tire studies could be made using nomographic charts, the existing theories of an elastic half space subjected to dynamic loads were extended for application to aircraft operations on unprepared runways. The development of the flotation parameter then incorporates the numerous tire variables and is based on the criteria of sinkage where sinkage is determined based on elastic theory.

As techniques become available which permit reliable predictions of total sinkage (elastic plus plastic) the concept of the flotation parameter which utilizes this total sinkage can become an effective design criteria for landing gear systems.

2. Development of the Flotation Parameter

a) Tire Characteristics

The numerous tire variables which influence sinkage have been previously summarized in Figure 2. Analysis of existing experimental data (1) has indicated that ply rating and tread pattern do not significantly influence tire performance. The tire inflation pressure, initial tire stiffness, and wheel load all influence the tire contact area, contact geometry, and contact stress distribution. If tire deflection (in per cent) is analyzed

in relation to contact area then the complex interaction between tire stiffness, inflation pressure, and load can be simplified. Figure 14 shows the variation of normalized contact area (A_1/A_2) with normalized tire deflection (d_1/d_2). In preparing Figure 14, data giving tire contact area at several deflections for a particular tire was used. Contact area and tire deflections were normalized so that data from several sources (1, 7, 18) could be analyzed. Tire diameters between 30" and 70" are included which is the usual range for aircraft tires. Reference to Figure 14 indicates that an essentially linear relationship exists between normalized contact area and normalized tire deflection for the range of normalized tire deflections considered (0.3 to 2.5). This simplified relationship will permit comparison of tire performance at different deflection levels.

Information is notably lacking on the distribution of contact stress between tires and soil at different inflation pressures. Analysis of the limited information available (18) indicates that at lower inflation pressures (high tire deflection), the contact stress distribution tends to be uniform while at high inflation pressures, the contact stress distribution is parabolic with the peak stress occurring immediately beneath the center line of the tire. A region of transition for contact stress distribution will naturally lie between these two extremes. Existing data does not, however, permit a quantitative look at this transition region. The flotation parameter nomograph was developed for the single case of a uniformly distributed load. As additional information becomes available on contact stress distribution vs. tire deflection in the transition region, a correction factor can be incorporated into the flotation parameter.

The contact geometry between tires and soil has not been determined in detail. Table III summarizes a limited amount of data from two sources (8, 18), which indicates the contact geometry to be elliptical in shape.

TABLE III
Elliptical Contact Geometry

Tire	Inflation Pressure (psi)	Major Axis=a	Minor Axis=b	Ratio = a/b	Soil Type
11.00-20, 12 PR	15	18.5"	12.5"	1.48	Sand
11.00-20, 12 PR	15	19.0"	12.5"	1.52	Clay
11.00-20, 12 PR	30	12.0"	7.0"	1.72	Rigid
9.00-14, 8 PR	15	9.3"	6.3"	1.46	Rigid

As indicated in Table III, the contact shape tended to be elliptical with ratios of the major to minor principal axes ranging from 1.4 to 1.7. This limited data indicates that the contact geometry does not differ significantly from a circular contact area, and consequently, since only maximum vertical sinkage is required, circularly loaded areas were used in the development of the flotation parameter.

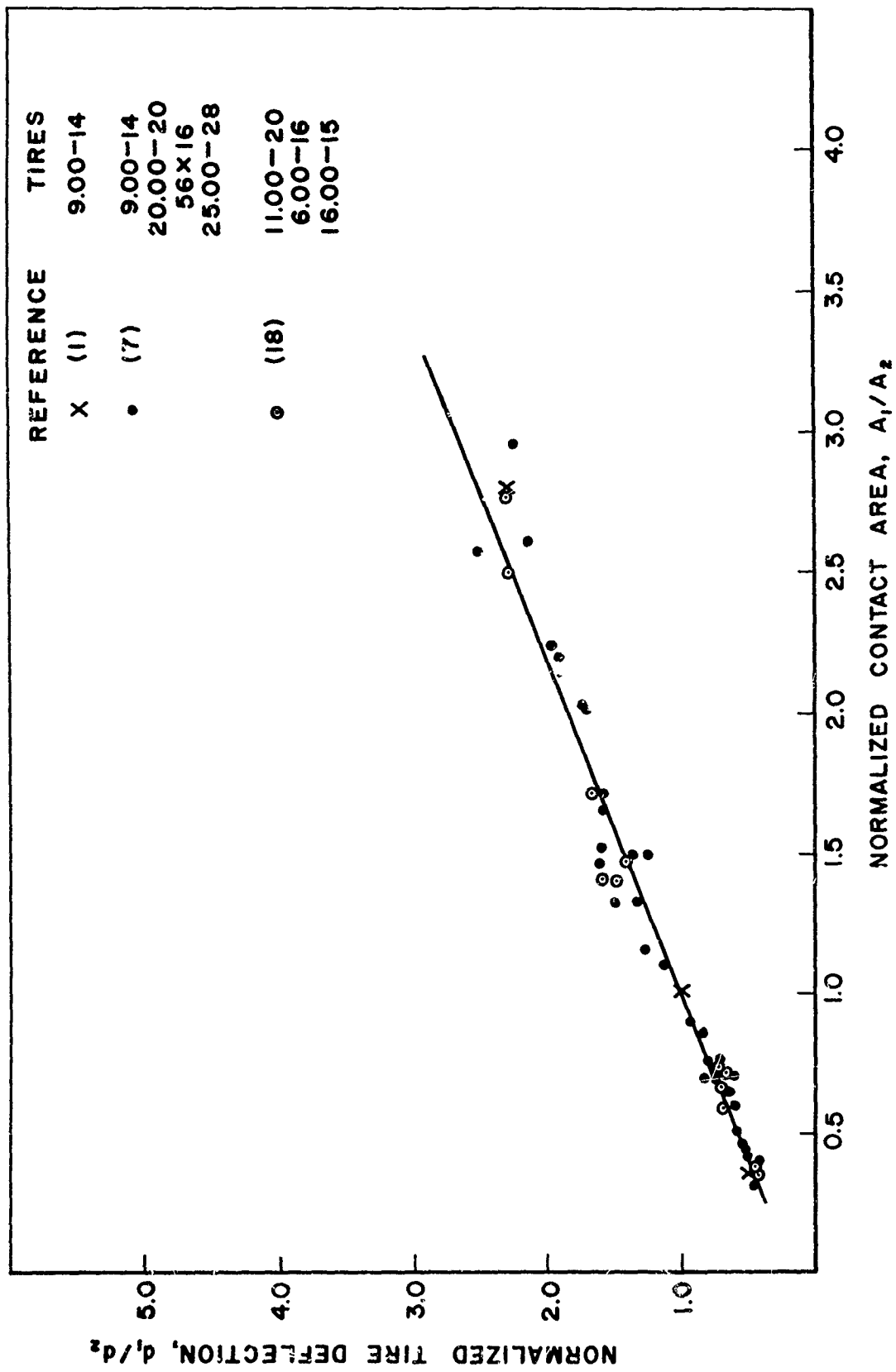


Figure 14 Normalized Tire Deflection vs Contact Area Ratio

b) Ground Loading

The determination of the load time history at a point in a semi-infinite half space (soil medium) due to aircraft loading is of considerable importance in analyzing the load-sinkage relationship for moving aircraft wheels. The dynamic ground sinkage depends not only on the peak load but also on the shape and duration of the load pulse. The ground surface loading can be thought of as having two components, vertical and horizontal (shear or drag) which influence the sinkage of the aircraft tire into the soil (see Figure 3). Table IV summarizes the relative magnitude of each of these components in defining sinkage for the different types of aircraft loadings on soil.

TABLE IV
Influence of Component Loading on Sinkage

Type of Loading	Components of Resultant Ground Loading	
	Vertical	Horizontal
Landing (Impact)	Major	Minor
Taxiing (Dynamic) Region 2	Major	Minor
Takeoff (Dynamic) Velocity Range	Major	Minor
Braking (Dynamic)	Major	Major

Reference to Figure 5 indicates that in most instances the ratio of the drag force to the vertical force is one-quarter or less for taxiing and takeoff operations. Since the flotation parameter is to be utilized for comparative purposes only, and noting that the major factor in vertical sinkage is the vertical load, the flotation parameter was developed based on vertical loadings. Little information is available concerning the shape, duration, and magnitude of the ground loading for landing situations and consequently the flotation parameter nomograph is related only to taxiing and takeoff operations. The impact landing and braking loading conditions are to be studied in a subsequent phase of the research program.

Considerable information is available on the load-time histories at a point in a semi-infinite half space under moving wheel loads from research work in flexible pavements and soil mechanics. Experimental measurements of load-time histories by use of load cells embedded in flexible pavements and in soil for rolling wheels provides an excellent source for defining the expected ground loading conditions in the path of an aircraft wheel for taxiing and takeoff.

Figure 15 shows several experimentally measured load-time histories (19, 20) which are typical of embedded load cell measurements. For comparison purpose, a half sine wave has been superimposed on the actual load-time trace. There is considerable similarity between the half sine wave and the actual load-time trace. Based on such comparisons, it has been common practice to assume that the load-time history at a point

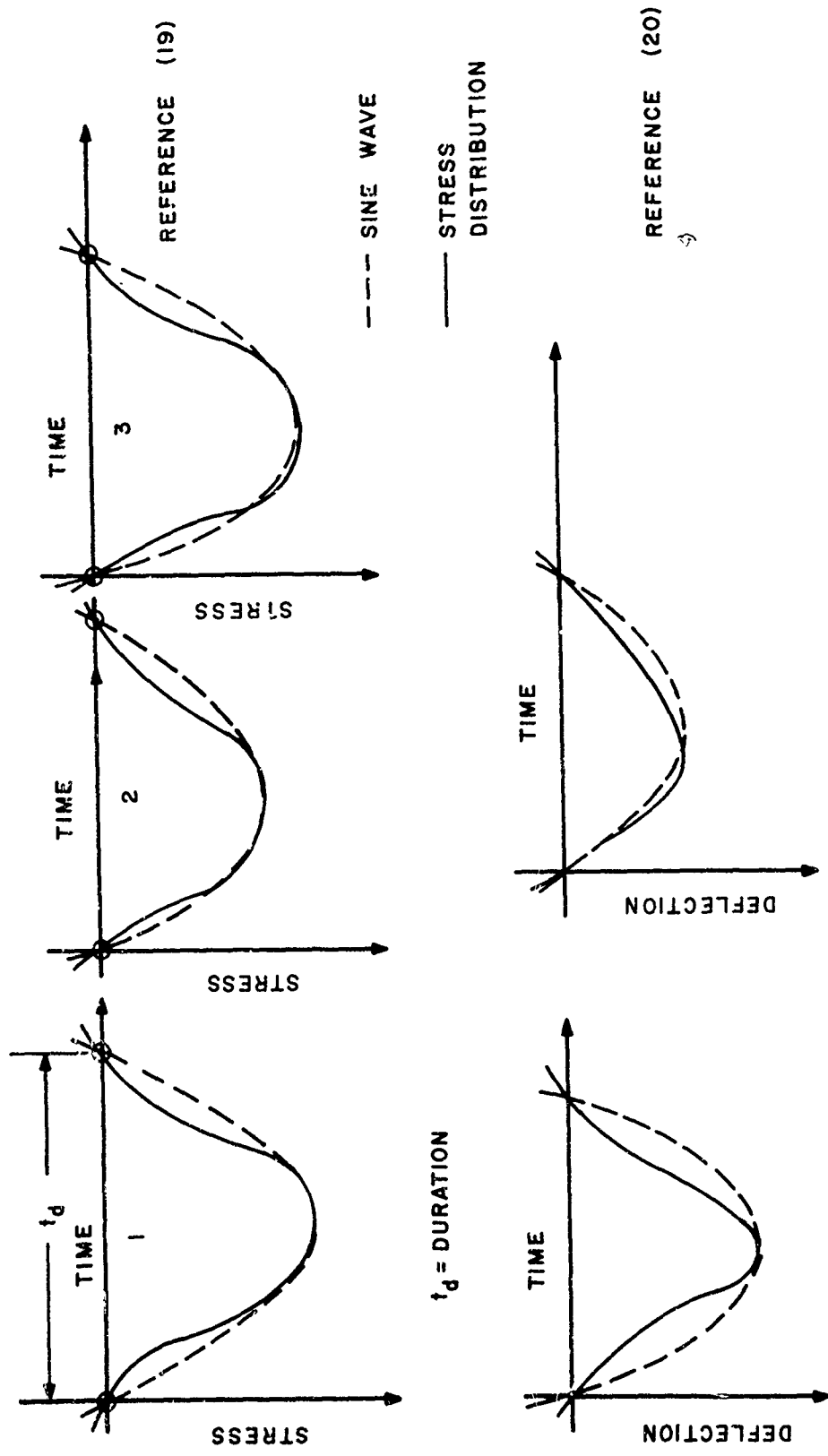


Figure 15 Load-Time History in Soil Due to Moving Wheel

in a soil medium or flexible pavement under moving wheel loads can be adequately approximated by a half sine wave (compressional loading). It has further been shown that the duration of the half sine wave loading is directly related to the speed of the traversing wheel. Table V summarizes wheel velocity-loading duration information currently available as developed from research work in soil mechanics and flexible pavements.

TABLE V
Velocity-Duration Relationship

Horizontal Wheel Velocity (knots)	Duration of Compressional Wave (sec.)	Reference
60	0.02 to 0.05	21, 22
30	0.11 to 0.14	22, 23
4	0.85 to 1.00	22, 23

Based on the above detailed experimental information, the load-time history at a point in the soil medium subjected to dynamic loading by an aircraft wheel will be represented by a half sine wave loading pulse. On a preliminary basis, Table V will be utilized for relating horizontal ground velocity to the loading duration.

c) Dynamic Soil Response

The response of a semi-infinite soil mass under dynamic loading has been determined on the assumption of the soil being a homogenous elastic medium (24, 25). Recent theoretical work by Richart and Whitman (26, 27) has demonstrated that for determining the relationship between load and soil response (vertical sinkage), that the dynamic behavior of the system can be adequately represented as a single degree of freedom lumped parameter system as indicated in Figure 16. The viscous damping component as represented by the dash pot in the model primarily reflects the damping action due to the dispersion of the elastic waves throughout the soil medium. The differential equation of motion for the model shown in Figure 16 for uniform loading is given by

$$m\ddot{Z} + c_1 \dot{Z} + k_1 Z = P(t) \quad (41)$$

where

m = equivalent mass of gear-wheel system

$$c = \frac{kr}{V_s}$$

$$k = \frac{\pi Gr}{(1 - \mu)}$$

and

- μ = Poisson's ratio
- r_o = radius of circularly loaded area
- G = soil shear modulus
- c_1, k_1 = parameters defined in Appendix II

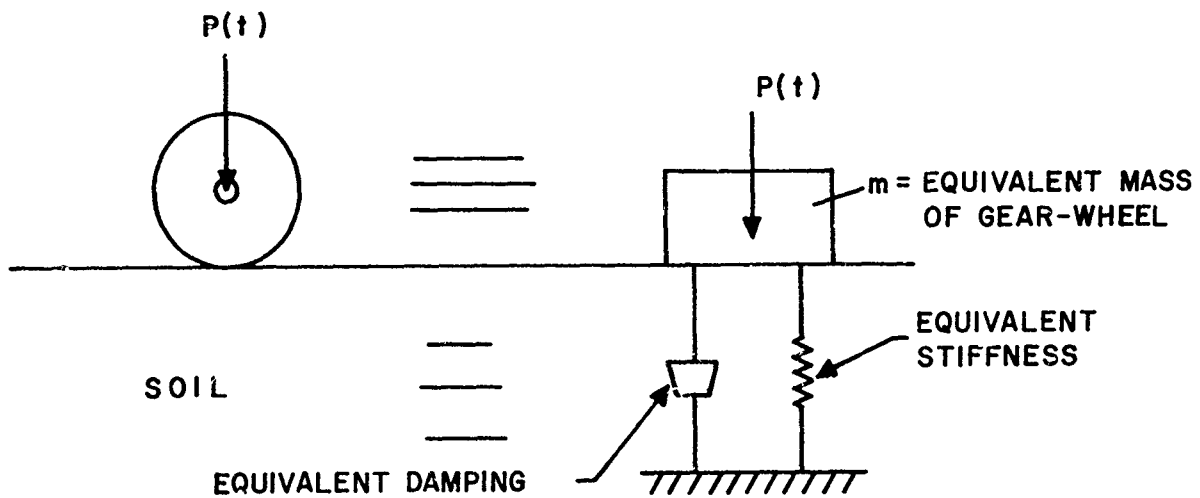


Figure 16 Half Space Mathematical Model (Elastic System)

The forcing function $P(t)$ is the time dependent vertical force. The solution of Equation (41) for a steady state harmonic loading,

$$P(t) = P_o \sin \omega t \quad (42)$$

where

P_o = peak amplitude of harmonic force

ω = angular frequency of steady state motion

is given by

$$Z(t) = \frac{P_o}{k} M \sin(\omega t + \phi) \quad (43)$$

where

$$M = \frac{1}{\sqrt{(1 - Ba_o^2)^2 + (c_1 a_o)^2}}$$

$$B = \text{mass ratio} = \frac{1 - \mu}{\pi} \cdot \frac{m}{\rho r_o^3}$$

ρ = mass density of soil

$$a_o = \text{frequency ratio} = \omega r_o \sqrt{\rho/G} = \frac{\omega r_o}{V_s}$$

$$\phi = \tan^{-1} \left(\frac{c_1 a_o}{1 - B a_o^2} \right)$$

and

$$V_s = \text{shear wave velocity}$$

As indicated previously, the aircraft tire is moving with a horizontal velocity across the soil medium. Consequently, the loading function $P(t)$ is a transient pulse in the form of a half sine wave of duration, t_d (see Figure 15). Presently available solutions are for steady state harmonic loading functions as indicated by Equation 43; however, Richart (26) has suggested a method of solution for transient loadings by use of Fourier analysis. By determining a Fourier series of loading functions which approximate the transient loading, and using the principle of superposition to add together the individual displacement solutions, the sinkage response is given in the form

$$Z(t) = \frac{P_o}{k} \sum_{n=0}^N M_n \sin(\omega_n t + \phi_n - \Psi_n) \quad (44)$$

where

Ψ_n = phase relationship between the individual frequency components

Computer programs were written to determine the maximum sinkage under a half sine wave transient loading for the variables of load duration (t_d), soil properties (μ , G , ρ), mass (m), and peak amplitude of load (P_o). The results were then used to develop the flotation parameter nomograph. The full details of the transient loading solution, together with the computer program, are given in Appendix II.

3. Flotation Parameter

Flotation is defined as the ability of the soil to support the load induced through the contacting element. The flotation parameter (F) is designed to absorb the numerous tire variables into a single parameter for comparative tire (or contacting element) studies based on flotation. The criteria for comparison of flotation in determining flotation parameters is sinkage. The flotation parameter nomograph shown in Figure 17 is based on:

- (1) The complex interrelationship of the tire variables can be simplified through the relationship of Figure 14.

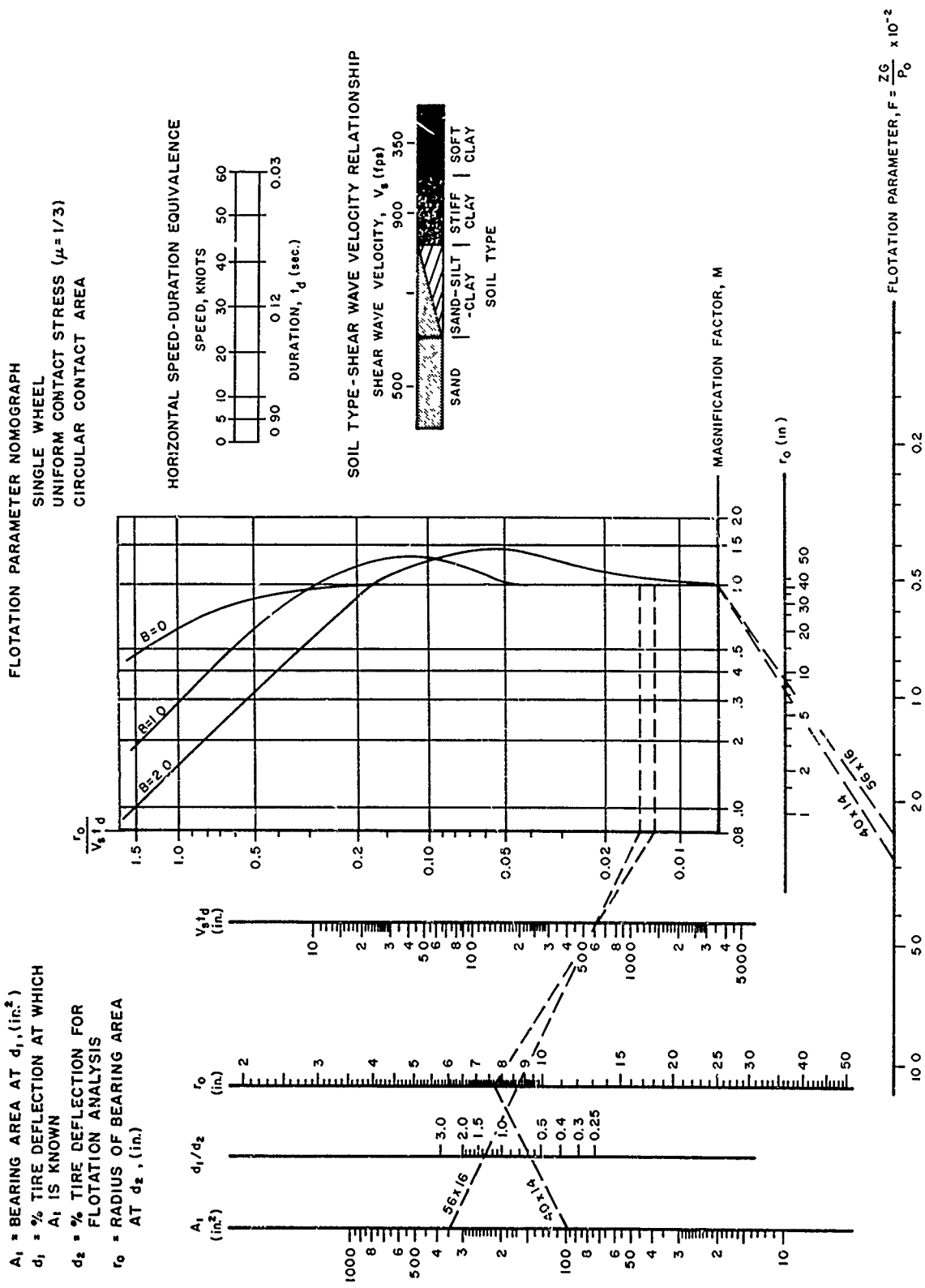


Figure 17 Flotation Parameter Nomograph

- (2) The contact stress is assumed to be uniform. *
- (3) The contact area is assumed to be circular. *
- (4) The loading at a point in the soil mass due to the moving wheel is in the form of a half sine wave transient load of duration, t_d .
- (5) The soil mass is assumed to be elastic.
- (6) The mass of the gear-wheel is incorporated through the mass ratio parameter, B. If $B = 0$, then only a forcing function exists at the ground surface.

Example of Use of Nomograph

Problem 1 Compare the relative flotation characteristics of the 56 x 16 tire to the 40 x 14 tire for both tires operating at 30% tire deflection (d).

Known Information

Clay soil, shear wave velocity, $V_s = 250$ fps,

horizontal wheel velocity = 25 knots, $t_d = 0.20$ sec,

the 56 x 16 tire has a known bearing area of 340 in.² at $d = 40\%$

the 40 x 14 tire has a known bearing area of 97 in.² at $d = 20\%$

Use $B = 0$

Solution by Nomograph

56 x 16 tire, $D = 55.7$ "

$$(1) \quad d_1/d_2 = 40/30 = 1.33$$

$$(2) \quad V_s \cdot t_d = 250 \times 12 \times 0.2 = 600$$

(3) Intersect 340 in.² (A_1) with $d_1/d_2 = 1.33$ which gives r_o at $d = 30\%$ of 8.8".

(4) Intersect $r_o = 8.8$ " with $V_s \cdot t_d$ of 600 to get $\frac{r_o}{V_s \cdot t_d} = 0.015$

(5) Move horizontally to intersect $B=0$ curve which gives $M = 1.0$

(6) Intersect $M = 1.0$ with $r_o = 8.8$ " to get the flotation parameter $F_{56 \times 16} = 2.5$

* Adjustments can be made to reflect more exact conditions, if experimental data becomes available which indicates such requirements.

40 x 14 tire, $D = 39.3''$

$$(1) \quad d_1/d_2 = \frac{20}{30} = 0.67$$

$$(2) \quad V_s \cdot t_d = 250 \times 12 \times 0.2 = 600$$

$$(3) \quad \text{Intersect } 97 \text{ in.}^2 (A_1) \text{ with } d_1/d_2 = 0.67 \text{ which gives } r_o = 7.7''$$

$$(4) \quad \text{Intersect } r_o = 7.7'' \text{ with } V_s \cdot t_d \text{ of } 600 \text{ to get } \frac{r_o}{V_s \cdot t_d} = 0.013$$

$$(5) \quad \text{Move horizontally to intersect } B=0 \text{ curve which gives } M = 1.0$$

$$(6) \quad \text{Intersect } M = 1.0 \text{ with } r_o = 7.7'' \text{ to get the flotation parameter } F_{40 \times 14} = 2.9$$

The 56 x 16 tire has higher flotation characteristics since it has less sinkage,

$$F_{56 \times 16} < F_{40 \times 14}$$

Relating the flotation to drag by use of Figure 5, would indicate an even higher relative flotation rating for the 56 x 16 tire since drag varies with the sinkage ratio, (Z/D) , and $D_{56 \times 16}$ is larger than $D_{40 \times 14}$, thus:

$$F.I._{56 \times 16} = \frac{F_{56 \times 16}}{D_{56 \times 16}} < \frac{F_{40 \times 14}}{D_{40 \times 14}} = F.I._{40 \times 14}$$

where

F.I. = flotation index

4. Summary

The nomograph shown in Figure 17 is an attempt to develop the concept of a flotation parameter in order to permit comparative flotation studies among landing gear systems. By using Figure 5 with the flotation parameter nomograph, comparison studies can also be made based on the flotation index. It does not provide completely adequate comparisons at the present time, since the sinkage is based solely on elastic theory while total sinkage of an aircraft tire involves both elastic and plastic deformations. As reliable techniques become available for predicting sinkage, the nomograph can be suitably modified to reflect these techniques and can provide the landing gear design engineer with considerable flexibility in analyzing flotation with the following objectives:

- (1) Comparative tire flotation studies where the soil and loading conditions are constant (see example problem #1).
- (2) Comparison of performance of a tire on different soil types.
- (3) Design of landing systems and contacting elements for reduced sinkage.
- (4) Selection of tires to reduce sinkage.
- (5) Determination of increased flotation with increasing tire deflections.
- (6) Comparative studies of drag magnitudes for the region two velocity range (see example problem #1).
- (7) Development of operational criteria for aircraft at specific landing sites.

These comparative studies conducted by use of a flotation parameter nomograph based on total sinkage will lead ultimately to a comparison of the relative merits of landing gear configurations with regard to their flotation capability on semi- and unprepared soil (relative design merit index).

SECTION VI

AIRCRAFT OPERATION CAPABILITY (SUITABILITY OF SITE)

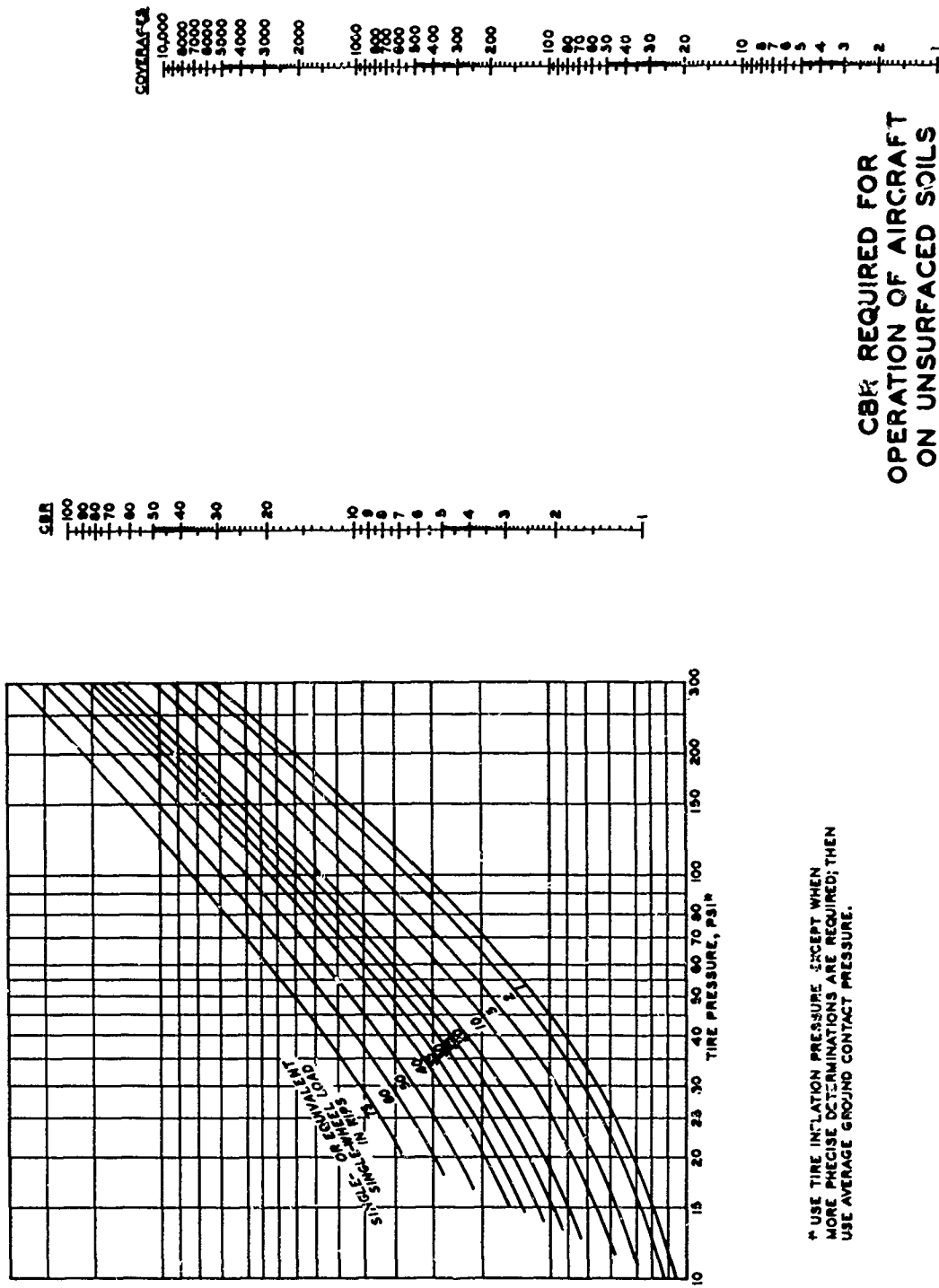
1. Failure Criteria

Determination of the capability of aircraft to operate on semi- and unprepared sites is generally made based on performance and is expressed as the number of coverages that can be carried out previous to failure (coverage is defined as sufficient passes of load tires in adjacent tire paths to cover a given width of surface area one time). Current Air Force standards specify the failure criteria as occurring when permanent rutting of clay soil exceeds 3 inches. The Army (9), in a recent experimental research investigation of aircraft tires operating on unprepared surfaces, utilized a failure criteria of 3 inches permanent deformation or 1.5 inches elastic deformation. The results of this research led to a modified "Unsurfaced Soil Strength Requirements" nomograph for determining the allowable number of aircraft tire coverages on forward airfields. For reference purposes this nomograph, which includes the variables of load, tire inflation pressure, and CBR, is shown in Figure 18. For multiple wheel arrangements an equivalent single wheel load is determined, based on Figure 19, to account for the effects of adjacent wheels as related to tire spacing.

Several limitations exist in the use of the strength requirements nomograph. The relationships developed are based on experimental data from tire tests primarily on "buckshot" clay soil. The recent modifications were made from test data on Buckshot clay which exhibits a high degree of elastic response. Consequently, as noted by the Air Force (28), the use of the nomograph for determining the number of operations is applicable only to heavy clay soils. Also, the distribution of loads used in defining coverage by the Army (9) often do not apply in forward airfield situations since the limited width airfields restrict aircraft operations to the centerline of the airstrip. Recent returning pilots from Vietnam who have operated C-123 and C-130 aircraft on unprepared airstrips report satisfactory operations on unprepared airstrips with rut depths up to five inches. Additionally, pilots have indicated the tendency to continually land aircraft in the centerline rut due to the limited airfield widths normally encountered in forward areas. The present criteria also does not include braking, turning, or landing impact effects.

2. Unified Approach

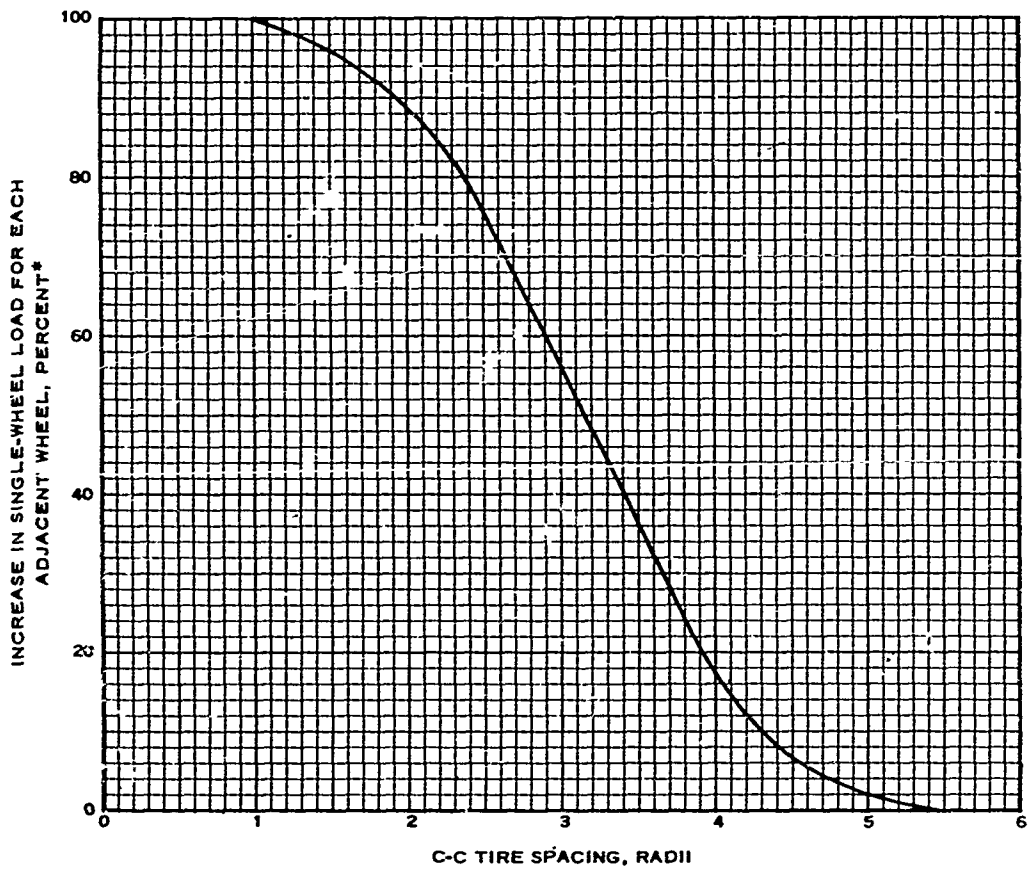
The problem of determining aircraft capability to operate at a site for aircraft operations clearly involves the relationship between permanent rut depth, roughness, and steering ability in addition to required runway lengths. The combination of initial roughness with subsequent permanent



CBR REQUIRED FOR OPERATION OF AIRCRAFT ON UNSURFACED SOILS

* USE TIRE INFLATION PRESSURE EXCEPT WHEN MORE PRECISE DETERMINATIONS ARE REQUIRED; THEN USE AVERAGE GROUND CONTACT PRESSURE.

Figure 18 CBR Required for Operation of Aircraft on Unsurfaced Soils



* INCREASE IN LOAD ON A SINGLE WHEEL OF A MULTIPLE-WHEEL GEAR TO ACCOUNT FOR EFFECTS OF ADJACENT WHEELS OF THE MULTIPLE-WHEEL GEAR IN ARRIVING AT AN EQUIVALENT SINGLE-WHEEL LOAD.

Figure 19 Equivalent Single-Wheel Load Adjustment Curve for Unsurfaced Soils

deformations defines the roughness of the airstrip for subsequent operations. Figure 20 shows the interrelationship of these factors in the development of a unified approach to aircraft operations capability and flotation. Since different types of aircraft undergo different dynamic structural responses when traversing the same rough terrain, the suitability should be related to specific types of aircraft. Until either additional full scale testing results become available on accepted tolerances of aircraft to rough terrain or until more accurate sinkage prediction techniques are developed, the capability of an aircraft to operate at a site cannot be fully defined.

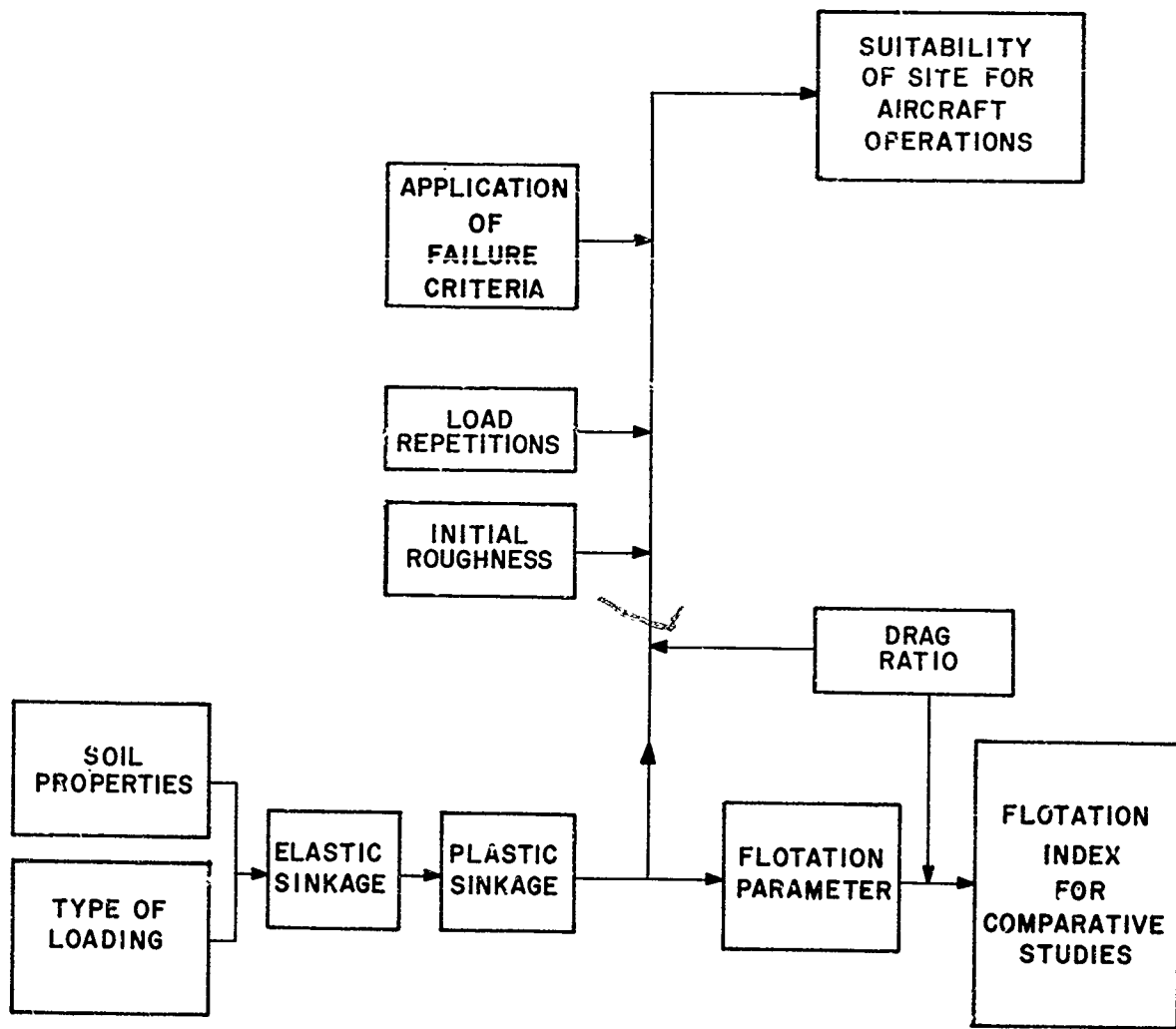


Figure 20 Unified Approach: Flotation Parameter-Aircraft Operation Capability

SECTION VII

CONCLUSIONS AND RECOMMENDATIONS FOR RESEARCH

1. Conclusions

In general, the results of the initial phase of the research effort including the literature review, have shown that the effects of such variables as soil type, speed, tire size, and other factors have not been completely defined in relation to the flotation of aircraft tires on soil. Those variables which significantly effect the landing gear-soil interaction phenomena have been identified. A review of existing flotation and mobility data has shown that:

- (1) There are at least three velocity regions for which the drag ratio exhibits distinct characteristics.
- (2) In the region two velocity range, the drag ratio (R/P) is directly proportional to the sinkage ratio (Z/D) for single tires.
- (3) Information is lacking on those variables which define the drag ratio response in the region three velocity range.
- (4) Little information is available which shows the effect of landing impact, braking (including antiskid system operation), and turning, on flotation and operation capability.

Since sinkage has been shown to be a significant variable in defining flotation, a review of the existing sinkage studies indicated three currently used sinkage prediction methods (models). The results of the comparative study between these sinkage prediction equations under identical soil, geometry, and loading conditions showed considerable difference in the magnitude of sinkage between methods. While the comparative study was based on a correlation of soil parameters (k_c , k_ϕ , n , C.I., G , and CBR), the result of the comparison together with the review of existing literature indicates that the accuracy of sinkage prediction utilizing present techniques is in the range of $\pm 50\%$ to $\pm 100\%$. In spite of the marked differences in the magnitude of sinkages predicted by the different equations for similar conditions, all the sinkage analysis equations indicate clearly the quantitative changes in flotation (sinkage and drag) with changes in the variables of tire deflection (d), tire diameter (D), and tire width (b). For example, by increasing the tire deflection of a 20.00-20 tire from 20% to 30% in a clay soil (CBR=2), an approximate decrease of 50% results in the magnitude of drag. Until more accurate sinkage prediction techniques are developed, particularly in defining the deformability response of soil to dynamic loads, suitable prediction of flotation response for determining the capability of aircraft to operate from a site cannot be made.

In order to meet the requirements of landing gear design engineers for the development of high flotation tires and landing gear systems based on a comparative evaluation, the concept of a flotation parameter and flotation index which ultimately should lead to a relative design merit index was developed. While the present flotation parameter utilizes elastic theory in defining soil response, as sinkage prediction techniques become available which include elastic and plastic deformation (total sinkage), the flotation parameter nomograph can be suitably modified to reflect total sinkage. The resulting modified nomograph could be a powerful tool in the comparative evaluation of landing gear systems for operation on semi- and unprepared soil.

2. Recommendations for Research

The review of the landing gear-soil interaction problem has shown several research deficient areas. These required research areas are summarized as follows:

a. Development of an accurate and reliable sinkage model incorporating load, geometry, and soil conditions. The extension of present techniques in finite element analysis, with a suitable yield criterion for soil to reflect the plastic deformation of soil, for application to the aircraft tire-soil interaction problem should lead to a more reliable sinkage prediction technique. In order to effectively develop the sinkage analysis, suitable correlations should be made between the sinkage prediction technique and experimental data from a controlled sinkage test program.

b. Further investigation of the drag ratio-velocity spectrum for the region three velocity range and higher velocities. Efforts, both theoretical and experimental, should be directed at the development of a drag ratio equation as related to the significant variables.

c. More reliable determination of twin (spacing) and tandem effects as related to flotation for aircraft wheels on soil (sand to clay).

d. Evaluation of the influence of braking, turning, and landing impact effects on surface roughness and flotation.

e. Extension of the present flotation parameter (F) and flotation index ($F.I.$) to a nomograph based on total sinkage for comparative studies and rating of present and proposed aircraft tires and landing gear systems.

On a more limited basis, investigation into the following areas could provide considerable additional insight into the interaction response between soil and aircraft tires:

f. Tire contact pressure distribution and contact geometry effects on flotation in soil.

g. Hydroplaning phenomena as related to tire and soil conditions.

h. Additional evaluation of the failure criteria for defining the capability of aircraft to operate from a site.

REFERENCES

1. Freitag, Dean R. Wheels on Soft Soils, an Analysis of Existing Data Technical Report No. 3-670, U.S. Army Corps of Engineers, WES, Vicksburg, Mississippi, January 1965.
2. Nuttal, C. J., Jr. A Dimensionless Consolidation of WES Data on the Performance of Sand Under Tire Loads Technical Report No. 3-130, U. S. Army Corps of Engineers, WES, Vicksburg, Mississippi, December 1965.
3. Bekker, M. G., and Janosi, Z. Analysis of Towed Pneumatic Tires Moving on Soft Ground Report No. RR-6, LL-62, U. S. Army Land Locomotion Laboratory, Detroit, Michigan, March 1960.
4. Liston, Ronald A., et al. State of the Art Report on Off the Road Mobility Research Research Report No. 6, U. S. Army Land Locomotion Laboratory, Detroit, Michigan, November 1966.
5. Richmond, L. D., DeBord, K. G., and Fuller, J. R., "Aircraft Dynamic Loads from Substandard Landing Sites," Phase I Interim Technical Report D6-16190, The Boeing Company, Renton, Washington, November 1965.
6. "Aircraft Landing Gear Dynamic Loads from Operation on Clay and Sandy Soil," Monthly Status Summary Reports 6, 7, 8, 9, Lockheed-Georgia Company, Marietta, Georgia, September 1967 to January 1968.
7. Ladd, D., and Ulery, H., Jr., et al. Aircraft Ground-Flotation Investigation Parts II to XIX, AFFDL-TDR-66-43, Air Force Flight Dynamics Laboratory, Wright-Patterson AFB, Ohio, August 1967.
8. Freitag, D. R., Green, A. J., and Murphy, J. R., Jr. "Normal Stresses at the Tire-Soil Interface in Yielding Soils," Highway Research Record No. 74, 1964.
9. Ladd, D. and Ulery, J., Jr. Aircraft Ground-Flotation Investigation Part I, Basic Report, AFFDL-TDR-66-43, Air Force Flight Dynamics Laboratory, Wright-Patterson AFB, Ohio, August 1967.
10. Bekker, M. G., A Definition of Soil Trafficability Report No. 41, Land Locomotion Laboratory, Detroit, Michigan, June 1958.
11. Assur, A., "Locomotion Over Soft Soil and Snow," Paper No. 782F, Automotive Engineering Congress, SAE, Detroit, Michigan, January 1964.

12. Janosi, Z. Prediction of WES Cone Index by Means of a Stress-Strain Function of Soils Report No. 46, Land Locomotion Laboratory, Detroit, Michigan, February 1959.
13. Sperry, Jack, AFFDL, WPAFB, letter of communication to David C. Kraft, University of Dayton, August 1967, subject: "Mechanical Tire Property Nomographs".
14. Scala, A. J., "Simple Methods of Flexible Pavement Design Using Cone Penetrometers," 2nd Australian and New Zealand Conference on Soil Mechanics and Foundation Engineering, 1956.
15. Christian, J. T. Two Dimensional Analysis of Stress and Strain in Soils Report No. 3-129, U. S. Army Corps of Engineers, WES, Vicksburg, Mississippi, December 1966.
16. Reese, L. C. and Vallabhan, C. V. G., Finite Element Method Applied to Problems in Stresses and Deformation of Soil NASA CR 66318, University of Texas, Department of Civil Engineering, January 1967.
17. Yong, R. N. and Osler, J. C. "On the Analysis of Soil Deformation Under a Moving Rigid Wheel," Soil Mechanics Series No. 16, McGill University, Department of Civil Engineering and Applied Mechanics, Montreal, April 1966.
18. Freitag, D. R. and Green, A. J., Distribution of Stresses on an Unyielding Surface Beneath a Pneumatic Tire HRB, Bulletin No. 342, 1962.
19. Thompson, A. B. and Smith, Mary E. Wheeled Vehicles (M135), Lean and Fat Clay Technical Report No. 3-545, Report 2, U. S. Army Corps of Engineers, WES, Vicksburg, Mississippi, May 1960.
20. Coffman, B. S. and Kraft, D. C. The Structural Evaluation of Flexible Pavements Report No. 235-1, Engineering Experiment Station, The Ohio State University, 1964.
21. Dorman, G. M., "The Extension to Practice of a Fundamental Procedure for the Design of Flexible Pavements," International Conference on the Structural Design of Asphalt Pavements, University of Michigan, 1962.
22. Coffman, B. S. and Kraft, D. C., "A Comparison of Calculated and Measured Deflections for the AASHO Test Road," Proceedings, Association of Asphalt Paving Technologists, Vol. 33, Dallas, Texas, 1964.

23. Baker, R. F. "A Structural Design Procedure for Pavements," International Conference on the Structural Design of Asphalt Pavements, University of Michigan, 1962.
24. Arnold, R. N., Bycroft, G. N., and Warburton, G. B., "Forced Vibrations of a Body on an Infinite Elastic Solid," Journal of Applied Mechanics, ASME, September 1955.
25. Sung, T. Y., "Vibrations in Semi-Infinite Solids Due to Periodic Surface Loading," Journal of Soil Mechanics and Foundations Division, ASCE, January 1966.
26. Richart, F. E., Jr. and Lysmer, J. "Dynamic Response of Footings to Vertical Loading," Journal Soil Mechanics and Foundations Division, ASCE, January 1966.
27. Richart, F. E., Jr. and Whitman, R. V., "Comparison of Footing Vibration Tests with Theory," Journal Soil Mechanics and Foundations Division, ASCE, November 1967.
28. Gray, Donald H. and Williams, Donald E., "Evaluation of Aircraft Landing Gear Ground Flotation Characteristics for Operation from Unsurfaced Soil Airfields," SEFL Report 167, Launching and Alighting Division, Systems Engineering Group, Wright-Patterson AFB, Ohio. March 1967.

APPENDIX I

DRAG-SINKAGE EXPERIMENTAL DATA

TABLE VI

Drag-Sinkage Data, Reference (8), Single Wheel

Soil Type	Soil Properties	Tire Type	Tire Diameter (in.)	Tire Inflation Pressure (psi)	Wheel Load P (lbs)	Sinkage Z (in.)	Drag R (lbs)	Sinkage Ratio Z/D in 10^{-2}	Drag Ratio R/P in 10^{-2}	Wheel Configuration and Spacing	Report No.
Sand	CI = 30	11.00-20	42		3000	2.41	586	5.8	19.5		
Clay	CI = 45	11.00-20	42		3000	2.32	776	5.6	26.0		
Clay	CI = 41	11.00-20	42		3000	1.22	408	2.9	13.6		

TABLE VII

Drag-Sinkage Data, Reference (2), Single Wheel

Soil Type	Soil Properties	Tire Type	Tire Diameter (in.)	Tire Inflation Pressure (psi)	Wheel Load P (lbs)	Sinkage Z (in)	Drag R (lbs)	Sinkage Ratio Z/D in 10 ⁻²	Drag Ratio R/P in 10 ⁻²	Wheel Configuration and Spacing	Report No.
Sand		11.00-20	42					1.0	7.5		
"		"	"					2.0	9.0		
"		"	"					1.5	8.0		
"		"	"					2.5	16.5		
"		"	"					2.0	11.0		
"		"	"					2.5	11.0		
"		"	"					2.5	11.0		
"		"	"					7.0	23.5		
"		"	"					6.0	21.0		
"		"	"					3.5	13.0		
"		"	"					2.5	15.0		
"		"	"					3.0	15.5		
"		"	"					5.0	24.0		
"		"	"					9.0	28.0		
"		"	"					8.0	30.0		
"		"	"					8.3	22.0		
"		"	"					7.0	28.0		
"		"	"					9.5	31.0		
"		"	"					5.3	26.0		
"		"	"					7.5	25.0		
"		"	"					9.0	32.0		

TABLE VIII

Drag-Sinkage Data, Reference (3), Single Wheel

Soil Type	Soil Properties	Tire Type	Tire Diameter (in.)	Tire Inflation Pressure (psi)	Wheel Load P (lbs)	Sinkage Z (in)	Drag R (lbs)	Sinkage Ratio Z/D in 10 ⁻²	Drag Ratio R/P in 10 ⁻²	Wheel Configuration and Spacing	Report No.
Natural (mixed)	k _c 9.9	7.00-16	32	6	400	0.55	36	1.72	9.0		
"	"	"	"	9	400	0.70	38	2.20	9.5		
"	"	"	"	12	400	0.90	42	2.81	10.6		
"	"	"	"	15	400	1.20	50	3.75	12.5		
"	"	"	"	6	500	0.75	44	2.34	8.8		
"	"	"	"	9	500	0.88	45	2.75	9.0		
"	"	"	"	12	500	1.05	48	3.29	9.6		
"	"	"	"	15	500	1.38	57	4.31	11.4		
"	"	"	"	6	600	0.75	53	2.34	8.8		
"	"	"	"	9	600	0.93	48	2.91	8.0		
"	"	"	"	12	600	1.13	50	3.53	8.3		
"	"	"	"	15	600	1.38	62	4.31	10.3		
"	"	"	"	6	700	0.85	65	2.66	9.3		
"	"	"	"	9	700	0.95	62	2.97	8.9		
"	"	"	"	12	700	1.13	63	3.53	9.0		
"	"	"	"	15	700	1.35	66	4.22	9.4		
Sand	k _c 4.0	"	"	6	400	1.00	54	3.12	13.5		
"	"	"	"	9	400	1.40	65	4.37	16.2		
"	"	"	"	12	400	1.85	82	5.78	20.5		
"	"	"	"	6	500	1.05	77	3.28	15.4		
"	"	"	"	9	500	1.35	80	4.22	16.0		
"	"	"	"	12	500	2.00	85	6.25	17.0		
"	"	"	"	6	600	1.30	100	4.06	16.7		
"	"	"	"	9	600	1.75	117	5.45	19.5		
"	"	"	"	12	600	2.50	148	7.80	24.6		
"	"	"	"	6	700	1.50	121	4.20	17.2		
"	"	"	"	9	700	2.05	137	6.40	19.6		
"	"	"	"	12	700	2.65	172	8.28	24.6		
Artificial Soil	k _c 21.0	7.00-16	32	8	300	1.95	50	6.1	16.7		
"	"	"	"	8	400	2.30	90	7.2	22.5		
"	"	"	"	8	500	2.60	130	8.1	26.0		
"	"	"	"	8	600	2.75	170	8.6	28.5		

TABLE IX

Drag-Sinkage Data, Reference (7), Single Wheel

Soil Type	Soil Properties (CBR)	Tire Type	Tire Diameter (in.)	Tire Inflation Pressure(psi)	Wheel Load P(lbs)	Sinkage Z(in.)	Drag R(lbs)	Sinkage Ratio Z/D in 10^{-2}	Drag Ratio R/P in 10^{-2}	Wheel Configuration and Spacing	Report No.
Clay	6.7	56 x 16	56	100	35,000	1.5	2400	2.7	6.85	Single Wheel	XVIII-17
"	6.7	"	"	"	"	1.6	2800	2.9	8.00	"	"
"	9.2	"	"	"	"	0.8	1500	1.4	4.30	"	"
"	9.2	"	"	"	"	1.0	2000	1.8	5.71	"	"
"	9.2	"	"	"	"	0.8	2100	1.4	6.00	"	"
"	6.7	"	"	"	"	0.9	1500	1.6	4.30	"	"
"	6.7	"	"	"	"	0.9	3500	1.6	10.0	"	"
"	11.0	"	"	"	"	0.4	1200	0.7	3.43	"	"
"	11.0	"	"	"	"	0.4	1500	0.7	4.30	"	"
"	11.0	"	"	"	"	0.7	2000	1.25	5.72	"	"
"	9.2	"	"	"	25,000	1.0	800	1.7	3.20	"	VIII-7
"	9.2	"	"	"	"	1.2	1300	2.1	5.20	"	"
"	9.2	"	"	"	"	2.1	1600	3.75	6.40	"	"
"	3.9	25.00-28	68	25	"	0.4	700	0.59	2.80	"	IX-8
"	3.9	"	"	"	"	0.8	900	1.18	3.60	"	"
"	3.9	"	"	100	"	2.2	1600	3.24	6.40	"	"
"	4.6	"	"	60	"	0.7	1200	1.03	4.81	"	"
"	4.6	"	"	60	"	2.1	1600	3.1	6.41	"	"
"	4.7	"	"	40	"	1.0	700	1.4	2.80	"	"
"	4.7	"	"	40	"	1.1	700	1.6	2.80	"	"
"	5.0	"	"	30	"	1.4	1500	2.06	6.00	"	"
"	5.0	"	"	30	"	1.9	1300	2.8	5.20	"	"
"	7.8	"	"	100	"	1.1	700	1.6	2.80	"	"
"	7.8	"	"	"	"	1.0	800	1.5	3.20	"	"
"	8.4	34 x 9.9	34	"	19,000	1.0	1400	2.9	7.37	"	"
"	8.4	"	"	"	"	1.0	2300	2.9	12.10	"	"
"	8.4	"	"	"	"	0.8	2500	2.4	13.10	"	"
"	4.2	20.00-20	55	"	21,000	2.70	2400	4.9	11.5	"	"
"	4.2	"	"	"	"	1.20	2400	2.2	11.5	"	"
"	6.3	"	"	"	"	0.9	1300	1.65	6.20	"	"
"	6.3	"	"	"	"	0.7	1400	1.27	6.67	"	"
"	6.3	"	"	"	"	0.9	2300	1.65	11.0	"	"
"	7.5	"	"	"	"	0.7	900	1.27	4.30	"	"
"	7.5	"	"	"	"	0.3	900	0.55	4.30	"	"
"	7.5	"	"	"	"	0.7	1300	1.27	6.20	"	"
"	7.5	"	"	"	"	0.6	1100	1.10	5.24	"	"

TABLE X

Drag-Sinkage Data, Reference (7), Twin Wheel

Soil Type	Soil Properties (CBR)	Tire Type	Tire Diameter (in.)	Tire Inflation Pressure (psi)	Wheel Load P (lbs)	Sinkage Z (in.)	Drag R (lbs)	Sinkage Ratio Z/D in -10 ⁻²	Drag Ratio R/P in 10 ⁻²	Wheel Configuration and Spacing	Report No.
Clay	9.2	56 x 16	56	100	35,000	1.8	2300	3.20	6.57	Twin-35" c-c	IV-3
"	9.2	"	"	100	"	2.0	4250	3.60	12.20	"	"
"	"	"	"	"	"	1.9	2000	3.40	5.72	Twin-25" c-c	III-2
"	"	"	"	"	"	1.4	3240	2.50	9.25	"	"
"	9.8	"	"	100	"	0.8	1850	1.40	5.30	Twin-60" c-c	V-4
"	9.8	"	"	100	"	1.3	1950	2.30	5.57	"	"
"	9.8	"	"	100	"	2.3	3100	4.10	8.85	"	"
"	8.8	"	"	100	"	1.6	1950	2.80	5.57	Twin-45" c-c	IV-3
"	8.8	"	"	100	"	1.4	2250	2.50	6.43	"	"
"	9.0	"	"	100	"	2.8	4200	5.00	12.00	"	"
"	27	"	"	200	52,000	1.1	2450	2.00	4.70	Twin-37" c-c	II-1
"	27	"	"	200	"	0.2	1800	0.36	3.46	"	"
"	18	"	"	200	"	0.7	2250	1.25	4.32	Twin-24" c-c	"
"	9.0	25.00-28	68	100	60,000	9.9	2600	1.30	4.33	Twin-56" c-c	VII-6
"	9.0	"	"	100	"	1.1	3000	1.60	5.00	"	"
"	9.0	"	"	100	"	2.6	3800	3.80	6.34	"	"
"	4.8	"	"	50	35,000	1.2	1400	1.76	4.00	Twin-42" c-c	X-9
"	4.8	"	"	50	"	1.6	1750	2.36	5.00	"	"
"	4.8	"	"	50	"	1.4	2550	2.06	7.29	"	"
"	4.7	"	"	50	"	1.1	1600	1.60	4.57	Twin-58.5" c-c	XIII-13
"	4.7	"	"	50	"	1.3	1750	1.90	5.00	"	"
"	4.7	"	"	50	"	0.7	2100	1.03	6.00	"	"
"	4.5	"	"	50	"	0.6	1400	0.88	4.00	"	"
"	4.5	"	"	50	"	0.9	2000	1.30	5.70	"	"
"	4.5	"	"	50	"	0.6	2150	0.88	6.14	"	"
"	4.5	"	"	50	"	1.2	2300	1.80	6.58	"	"

TABLE XI

Drag-Sinkage Data, Reference (7), Multiple Wheel

Soil Type	Soil Properties (CBR)	Tire Type	Tire Diameter (in.)	Tire Inflation Pressure (psi)	Wheel Load P (lbs)	Sinkage Z (in.)	Drag R (lbs)	Sinkage Ratio Z/D in -10 ⁻²	Drag Ratio R/P in 10 ⁻²	Wheel Configuration and Spacing	Report No.
Clay	9.8	56 x 16	56	100	35,000	1.2	1850	2.10	5.30	Twin-Tandem	VI-5
"	9.8	"	"	100	"	2.1	2280	3.80	6.50	Twin-37", Tandem 60"	
"	11.0	"	"	100	"	0.7	1100	1.25	3.14	3-abreast	XII-11
"	11.0	"	"	100	"	0.9	1570	1.60	4.49	33" c-c-c	
"	10.0	"	"	100	"	0.8	900	1.40	2.58	3-abreast	
"	10.0	"	"	100	"	1.2	2260	2.10	6.46	27" c-c-c	
"	3.8	20.00-20	55	100	21,000	2.40	2360	4.36	11.20	12-wheel, 4 abreast	XIV-14
"	6.1	"	"	100	"	2.20	1120	4.00	5.34	30-1/4", 34-3/4", 30-1/4"	
"	10.0	"	"	100	"	0.68	640	1.24	3.04	3 in line	
"	10.0	"	"	100	"	0.40	610	0.73	2.90	123"-123" c-c-c	
"	4.4	"	"	55	"	1.4	700	2.55	3.33	12 wheel, 4 abreast	XVI-15
"	4.4	"	"	55	"	2.0	1020	3.64	4.86	34"-34"-34"	
"	8.1	"	"	55	"	0.4	550	0.73	2.62	c-c-c-c	
"	8.1	"	"	55	"	0.9	500	1.64	2.38	3 in line	
"	4.7	"	"	55	"	0.8	670	1.45	3.18	123"-123" c-c-c-c	
"	4.7	"	"	55	"	0.9	760	1.64	3.62	123"-123" c-c-c-c	
"	7.0	"	"	55	"	0.4	510	0.73	5.85	123"-123" c-c-c-c	
"	7.0	"	"	55	"	0.3	500	0.55	2.30	123"-123" c-c-c-c	
"	7.0	"	"	55	"	0.6	750	1.09	2.24	123"-123" c-c-c-c	
"	9.0	"	"	100	22,800	0.6	800	1.09	3.60	123"-123" c-c-c-c	XVII-16
"	9.0	"	"	100	"	0.7	800	1.26	3.80	123"-123" c-c-c-c	
"	9.0	"	"	100	"	0.6	920	1.09	4.38	123"-123" c-c-c-c	

TABLE XII
 Drag-Sinkage Data, Reference (5), Single Wheel

(data taken from mean line sinkage ratio and drag ratio relationship)

Soil Type	Soil Properties (CBR)	Tire Type	Tire Diameter (in.)	Tire Inflation Pressure (psi)	Wheel Load P(lbs)	Sinkage Z (in.)	Drag R(lbs)	Sinkage Ratio Z/D in 10^{-2}	Drag Ratio R/P in 10^{-2}	Wheel Configuration and Spacing	Report No.
								<u>Yuma Sand</u>			
								8.9	28		
								6.2	21		
								5.3	18		
								4.8	16		
								4.0	15		
								3.5	13		
								2.3	8.9		
								1.6	6.2		
								<u>Buckshot Clay</u>			
								4.8	16		
								2.7	11		
								1.9	8		
								1.3	6		
								0.93	4.9		
								0.77	4.2		
								0.60	3.6		

APPENDIX II
TRANSIENT LOADING SINKAGE ANALYSIS,
COMPUTER PROGRAM

The steady state response of a rigid body in contact with a semi-infinite elastic medium has been analyzed by a number of investigators (24, 25, 26). While there are four modes of motion (vertical, torsion, horizontal, and rocking) for a rigid body with a circular contact area, only the vertical mode is of interest at this time to the flotation problem. For a rigid body resting on a semi-infinite medium and using the assumptions of a circular contact area, a homogeneous, isotropic, and elastic medium, and only normal stresses transferred at the interface, the vertical displacement (sinkage) of the rigid body with a uniform contact stress for a harmonic loading of the form

$$P(t) = P_o e^{i\omega t} \quad (45)$$

is given by

$$Z = \frac{P_o}{Gr_o} (f_1 + if_2) e^{i\omega t} \quad (46)$$

where

$f_1 f_2$ = dimensionless functions dependent on Poisson's ratio (μ), and the frequency ratio (a_o)

P_o = peak amplitude of harmonic force

ω = angular frequency of steady state motion

t = time

G = soil shear modulus

$i = \sqrt{-1}$

r_o = radius of circularly loaded area

and

$$a_o = \frac{\omega r_o}{V_s}$$

where

V_s = shear wave velocity in soil

The values of f_1 and f_2 are given in Table XIII for a uniform contact stress.

More recently the work by Lysmer and Richart (26) has shown that by defining the quantities

$$k_1 = \frac{F_1}{F_1^2 + F_2^2} \quad (47)$$

$$c_1 = \frac{-F_2/a_o}{F_1^2 + F_2^2} \quad (48)$$

where

$$F_1 = \pi f_1 / (1 - \mu), \quad F_2 = \pi f_2 / (1 - \mu)$$

An analogy can be drawn between the response of the half space model and a simple single degree of freedom lumped parameter system (see Figure 16). Noting that the differential equation of motion for a weightless rigid body is given by

$$c_1 \frac{kr}{V_s} \dot{Z} + k_1 kZ = P_o e^{i\omega t} \quad (49)$$

where

$$k = \frac{\pi Gr_o}{(1 - \mu)}$$

and that by adding the inertia term ($m \neq 0$), the differential equation of motion becomes

$$m\ddot{Z} + c_1 \frac{kr}{V_s} \dot{Z} + k_1 kZ = P_o e^{i\omega t} \quad (50)$$

The values of c_1 and k_1 as developed from equations 47 and 48 are given in Table XIII. The solution of Equation 50 for a forcing function

$$P(t) = P_o \sin \omega t \quad (51)$$

is

$$Z = \frac{P_o}{k} M \sin(\omega t + \varphi) \quad (52)$$

where

$$M = \sqrt{\frac{1}{(k_1 - Ba_o^2)^2 + (c_1 a_o)^2}} \quad (53)$$

and

$$B = \text{mass ratio} = \frac{1 - \mu}{\pi} \frac{m}{\rho r_o^3} \quad (54)$$

$$\varphi = \tan^{-1} \frac{-c_1 a_o}{k_1 - Ba_o^2} \quad (55)$$

For transient loading phenomena, Lysmer and Richart (26) suggested a Fourier series analysis utilizing steady state solutions. Figure 21 shows a vertical loading in periodic form. The loading function is a sequence of identical pulses of alternating sign and duration, t_d . The pulses are uniformly spaced and periodic ($2jt_d$). By selecting the integer, j , large (large spacing between the pulses), the system will undergo free vibrations in response to each pulse. These free vibrations will damp out (large damping due to energy dispersion in the half space) previous to the loading by a subsequent pulse. In effect then the system's response will be as if its loading were a transient pulse. In this case the transient pulse has been selected as a half

sine wave of duration, t_d , and peak intensity, P_o . Putting the loading function in nondimensional form as indicated in Figure 22, the load pulse can be defined as:

$$P(t) = P_o \varphi(t/t_d) \quad (56)$$

Reference to Figure 21 indicates that the loading function is of the form:

$$f(t - jt_d) = -f(t) \quad (57)$$

Expanding the loading function (Equation 56) in a Fourier series, letting $u = t/t_d$, and noting the relationship of Equation 57 leads to the following equations for the Fourier series coefficients

$$a_n = \frac{1}{j} \left[\int_{-j}^{-j+1} \varphi(u) \cos \frac{n\pi u}{j} du + \int_0^1 \varphi(u) \cos \frac{n\pi u}{j} du \right] \quad (58)$$

$$b_n = \frac{1}{j} \left[\int_{-j}^{-j+1} \varphi(u) \sin \frac{n\pi u}{j} du + \int_0^1 \varphi(u) \sin \frac{n\pi u}{j} du \right] \quad (59)$$

which reduces to

$$a_n = \frac{2}{j} \int_0^1 \varphi(u) \cos \left(\frac{(2n+1)\pi u}{j} \right) \pi u du \quad (60)$$

$$b_n = \frac{2}{j} \int_0^1 \varphi(u) \sin \left(\frac{(2n+1)\pi u}{j} \right) \pi u du \quad (61)$$

The Fourier series developed from this loading function is then

$$P(t) = P_o \sum_{n=0}^N c_n \cos \left[\frac{(2n+1)\pi t}{j t_d} - \psi_n \right] \quad (62)$$

where

$$c_n = \sqrt{a_n^2 + b_n^2}$$

$$\psi_n = \tan^{-1} \frac{b_n}{a_n}$$

and

N is a large integer.

Using the principle of superposition as applied to Equation 52 for linear systems gives the following series for the vertical displacement (sinkage)

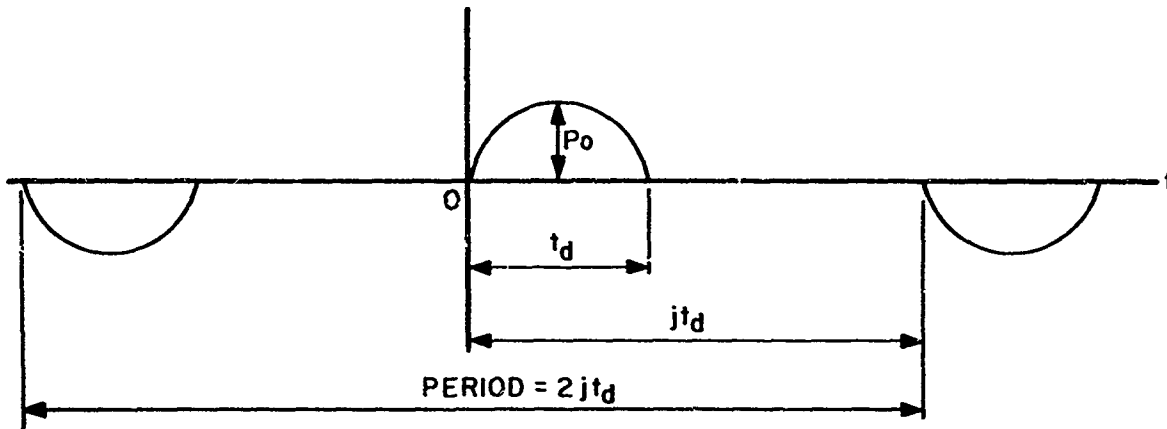


Figure 21 Periodic Loading Pulses

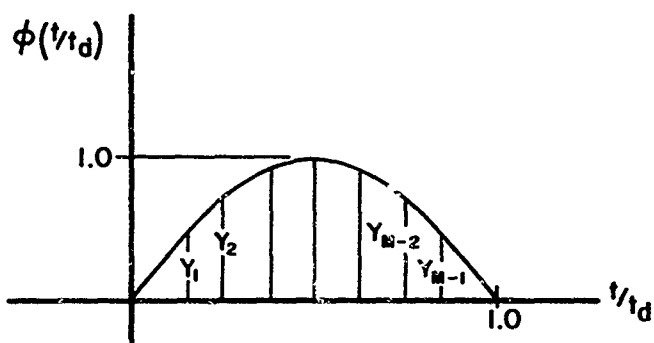


Figure 22 Dimensionless Loading Function (Half Sine Wave)

$$Z(t) = \frac{P_o}{k} \sum_{n=0}^N M_n \cos \left(\frac{2n+1}{j t_d} \pi t + \varphi_n - \psi_n \right) \quad (63)$$

where

$$M_n = \sqrt{\frac{1}{(k_{1n} - B a_{on}^2)^2 + (c_{1n} a_{on})^2}} \quad (64)$$

$$a_{on} = \frac{2n+1}{j t_d} \frac{r_o}{V_s} \quad (65)$$

$$\varphi_n = \tan^{-1} \left(\frac{-c_{1n} a_{on}}{k_{1n} - B a_{on}^2} \right) \quad (66)$$

The values of c_{1n} and k_{1n} can be determined from Table XIII based on a_{on} .

As indicated by Lysmer and Richart (26) most of the response is developed from the lower frequency contents and consequently a good approximation to the sinkage can be obtained for reasonably small values of N . An approximation to the number of terms required is given by (26)

$$N > \frac{(j t_d) V_s}{(2\pi r_o \sqrt{B\epsilon'})} \quad (67)$$

where ϵ' defines the required accuracy.

The determination of the sinkage, Z , through the series as expressed by Equation 63 requires the evaluation of a_n and b_n by the integral form of Equations 60 and 61. Since in the general case the load pulse as described by $\varphi(t/t_d)$ is not always a shape which can be described by a closed form equation, the loading function was specified as a segmented function as shown in Figure 22 and consequently this integration for evaluating a_n and b_n was carried out numerically.

Previous to numerical analysis, if the expressions for a_n and b_n are evaluated using product of variable integration techniques, then the resulting expressions become

$$a_n = \frac{2j}{(2n+1)^2 \pi^2} \int_0^1 \varphi''(u) \cos \left(\frac{2n+1}{j} \pi u \right) \pi u du \quad (68)$$

$$b_n = \frac{2j}{(2n+1)^2 \pi^2} \int_0^1 \varphi''(u) \sin \left(\frac{2n+1}{j} \pi u \right) \pi u du \quad (69)$$

where $\varphi''(u)$ is the second derivative of $\varphi(u)$. By expressing $\varphi''(u)$ by a finite difference equation where

$$\varphi''(u) = \frac{1}{(\Delta u)^2} (2Y_i - Y_{i-1} - Y_{i+1}) \quad (70)$$

and numerically evaluating the integrals for the pulse being split into M-equally spaced intervals, the expressions for the Fourier series coefficients are given by

$$a_n = \frac{2jM}{(2n+1)^2} \sum_{i=0}^M (2Y_i - Y_{i-1} - Y_{i+1}) \cos \left(\frac{(2n+1)i\pi}{jM} \right) \quad (71)$$

$$b_n = \frac{2jM}{(2n+1)^2 \pi^2} \sum_{i=0}^M (2Y_i - Y_{i-1} - Y_{i+1}) \sin \left(\frac{(2n+1)i\pi}{jM} \right) \quad (72)$$

Computer programs were written for evaluating Equations 63, 71, and 72 using an IBM 7044/7094 Direct Couple System located at Wright-Patterson Air Force Base for a half sine type pulse as indicated in Section V. The programming was accomplished using the dimensionless variables,

$\frac{r_o}{V_s t_d}$, and B in determining the sinkage, Z, and these results were utilized

in the development of the flotation parameter nomograph (see Figure 17). A complete listing for the computer program is given below.

Table XIII. Dimensionless Parameters - Uniform Loading Case

a_o	$-f_1$	f_2	F_1	F_2	c_1	k_1
0	0.21	0.0	0.99	0.000	0.62	1.00
0.25	0.205	0.03	0.96	0.141	0.62	1.00
0.50	0.20	0.065	0.94	0.305	0.63	0.97
0.75	0.185	0.09	0.87	0.42	0.63	0.93
1.0	0.16	0.115	0.75	0.54	0.64	0.88
1.5	0.115	0.150	0.54	0.71	0.61	0.64
2.0	0.06	0.175	0.28	0.83	0.55	0.36

TRANSIENT LOADING SINKAGE ANALYSIS

DOUBLE PRECISION SUMA,SUMB, EYE, MULT, ALF, BETA, PI, C, A, TEMP,
 2TEMP2,PHASE(1000),BEE(1000),DELT,PJM,YE,DD
 DIMENSION Y(50), TABLE(2,11)
 LOGICAL PNTSER,PNTDEL
 REAL MA

C *TABLE, GIVES C1 AND K1 VALUES FOR UNIFORM LOADING CASE
 C K1 VALUES, TABLE(1,I) IS C1 VALUES, TABLE(2,I)
 C MU = 1/3 IS ASSUMED FOR *TABLE
 C *Y, IS PULSE SHAPE FUNCTION -- HERE AN APPROXIMATION TO SINE
 DATA ((TABLE(I,J),I=1,2),J=1,9)/ 1.00, 0.62, 1.00, 0.62,
 2 0.55, 0.62, 0.91, 0.62, 0.76, 0.61, 0.76, 0.61,
 3 0.50, 0.58, 0.50, 0.58, 0.50, 0.55/
 4 (Y(I),I=1,23)/0.0,0.0,0.156435,0.309017,0.45399,0.587785,
 5 0.707107,0.809016,0.891012,0.915448,0.987689,1.0,
 6 0.987689,0.915448,0.891012,0.809016,0.707107,0.587785,0.45399,
 7 0.309017,0.156435,0.0,0.0

PI=3.1415926535897932
 GET PROBLEM PARAMETERS
 I READ(5,500) RRHD,Q,D,G,RO,MA,DELTA,FINAL,PNTSER,PNTDEL
 M=20

C INPUT DATA (FOR FORMAT SEE 500)
 C QO IS PEAK LOAD (LB.)
 C D IS PULSE DURATION (SEC)
 C G IS SHEAR MODULUS OF ELASTICITY (PSI)
 C RO IS FOOTING RADIUS (INCHES)
 C MA IS GEAR MASS (LB-SEC**2/IN)
 C DELTA IS STEP SIZE FOR TIME EVALUATION (SEC)
 C FINAL IS TERMINAL TIME (SEC)--INITIAL TIME ASSUMED = 0
 C PNTSER PRINT SERIES PARAMETERS IF PNTSER = T
 C PNTDEL PRINT DISPLACEMENTS TABLE IF PNTDEL = T
 C IN EITHER CASE AN F OR BLANK WILL SUPPRESS PRINTING

XXXXXX NMAX+1
 X X 2N-1
 C DELTA(T) = X BEE(N) COS(--PI*T + PHASE(N))
 X X J*0
 C XXXXXX N=1

C DELTA, AND DELTA, ARE OBTAINED BY TAKING NMAX+1 TERMS OF THE DERIVATIVES

```

C OF THE ABOVE SERIES.
C
C CALCULATE PARAMETER VALUES FROM INPUT DATA AND PRINT THEM
C THE FORMULA BELOW FOR CK(I,E,K) IS VALID FOR
C THE UNIFORM LOADING CASE WHEN MU = 1/3 (THAT VALUE OF MU HAS BEEN USE D TO
C SIMPLIFY THE CONSTANT FACTOR)
C IN GENERAL (UNIFORM LOADING) THE FORMULA IS.. CK=PI*G*RO/(1-MU)
  CK=1.5*PI*G*RO
  VS=SQRT(G/RRHU)
  B=MA*VS*VS/(CK*RO*RO)
  WRITE(6,505) Q0,D,G,RO,MA,CK,B,VS
C CHOOSE J AND NMAX AS INTEGERS .GT. EQNS. 84,85 RESP.
C EPSILON IS 0.05 ( TO CHANGE EPSILON, CHANGE THE 0.05 IN 9 AND 10 )
  9 J=2.0-(2.0+.0#B)*RO*ALOG10(0.05)/(VS*D)
  10 NMAX=1.0+VS*D*FLOAT(J)/(6.2831853*SQRT(0.05*B)*RO)
  WRITE(6,700) J,NMAX
  IF(J.GT.0) GO TO 11
  J=5
  GO TO 10
  11 DJ=D*FLOAT(J)
  RHO= RO/(VS*DJ)
  PJM=PI/FLOAT(J*M)
  EN=-1.0
  IF(.NOT.PNTSER) GO TO 12
  C HEADING FOR SERIES PARAMETER LISTING, IF REQUESTED (PNTSER IS T)
  WRITE(6,702)
  12 CONTINUE
  C CALCULATE PARAMETERS FOR NMAX+1 TERMS OF THE SERIES
  M=21
  NMAX=NMAX+1
  DO 50 N=1,NMAX
  EN=EN+2.0
  SUMA=0
  SUMH=0
  EYE=-PJM*EN
  YE=-EYE
  DO 40 I=1,M
  EYE=EYE+YE
  DD=2.0*DBLE(Y(I+1))-DBLE(Y(I))-DBLE(Y(I+2))

```

```

40  SUMA=SUMA+DD*DCOS(EYE)
    SUMB=SUMB+DD*DSIN(EYE)
    MULT=  FLOAT(2*J*(M-1))/((EN*PI)**2)
    ALF=MULT*SUMA
    BETA=-MULT*SUMB
    C=DSQRT(ALF*ALF+BETA*BETA)
    A=EN*PI*RHQ
    NEXT 4 CARDS GET K1 AND C1 FROM TABLE
    K=4.0*A+1.0
    IF(K.GT.9) K=9
    CONSTK=TABLE(1,K)
    C1=TABLE(2,K)
    TEMP=CONSTK-B*(A**2)
    TEMP2=-C1*A
    PHASE(N)=DATAN2(TEMP2,TEMP)+DATAN2(BETA,ALF)
    BEE(N)=C/DSQRT(TEMP2*TEMP2+TEMP*TEMP)
    IF(.NOT.PNTSER) GO TO 50
C   PRINT THE SERIES PARAMETERS, IF REQUESTED (PNTSER IS T)
    WRITE(6,600) N,ALF,BETA,C,BEE(N),A,PHASE(N),CONSTK
    CONTINUE
50  C   NOW EVALUATE SERIES FOR TIME=0 STEP DELTA UNTIL FINAL
    TIME=0
    MULT=90/CK
    DELMAX=0
    IF(.NOT.PNTDEL) GO TO 70
C   HEADING FOR DISPLACEMENT LISTING, IF REQUESTED (PNTDEL IS T)
    WRITE(6,601)
    GO TO 70
60  TIME=TIME+DELTA
    IF(TIME.GT.FINAL) GO TO 100
70  SUMA=0
    SUMAA=0
    SUMAAA=0
    EN=-PI/DJ
    ENINC=-2.0*EN
    DO 80 N=1,NMAX
    EYE=SUMA
    EN=EN+ENINC
    SUMB=EN*TIME+PHASE(N)

```

```

TEMP=DCOS(SUMB)
TEMP2=-BEE(N)*EN
SUMAA=SUMAA+TEMP2*DSIN(SUMB)
SUMAAA=SUMAAA+TEMP2*EN*TEMP
SUMA=SUMA+BEE(N)*TEMP
EC=MULT*SUMA
C  CALCULATE VELOCITY AND ACCELERATION FROM SERIES FOR DISPLACEMENT
ECC=MULT*SUMAA
ECCC=MULT*SUMAAA
DELMAX=AMAX1(EC,DELMAX)
IF(.NOT.PNTDEL) GO TO 60
WRITE(6,610) TIME,EC,ECC,ECCC
GO TO 60
100  RATIO=DELMAX/MULT
      RMULT=MULT
C  DELMAX IS THE LARGEST DELTA(T) WHICH HAS BEEN CALCULATED
WRITE(6,611) DELMAX,RMULT,RATIO
GO TO 1
500  FORMAT(2F10.5,F4.1,F7.1,F7.2,F7.1,5X,2F5.3,2L1)
505  FORMAT(16H1TEST PARAMETERS/ 20H RHO=1.7E-4      QO=, F8.1, MU=1/3
      15H LR.  DURATION=F4.1,9H SEC  G=,F6.1,14H PSI
      /5H RO=,F6.2,12H IN.  MASS=,F5.1,7X,2HK=,E13.7,
      7H      B=,E13.7,5H VS=,E13.7)
600  FORMAT(1H , I4, 6D20.12,F5.2)
601  FORMAT(38H0 TIME      DELTA(TIME)  DELTA(TIME) ,
      15H DELTA,(TIME) )
610  FORMAT(1H ,F7.4,3E15.6)
611  FORMAT(1H0, 11HDELTA(MAX)= , E14.6,17H DELTA(STATIC)=,
      2  E14.6, 29H DELTA(MAX)/DELTA(STATIC) =, E14.6)
700  FORMAT(5H J = ,I5, 7H NMAX = ,I5)
702  FORMAT(5H1 N, 17X,3HALF,15X,5H-BETA,19X,1HC,12X,8HLITTLE B,
      2  12X,8HLITTLE A, 11X,9HPHI + PSI , 5H CONK )
      END

```

Unclassified
Security Classification

DOCUMENT CONTROL DATA - R&D		
<i>(Security classification of title, body of abstract and indexing annotation must be entered when the overall report is classified)</i>		
1 ORIGINATING ACTIVITY (Corporate author) University of Dayton Research Institute Dayton, Ohio 45409		2a REPORT SECURITY CLASSIFICATION
		2b GROUP
3 REPORT TITLE Analytical Landing Gear - Soils Interaction - Phase I		
4 DESCRIPTIVE NOTES (Type of report and inclusive dates) Final Report, 15 May 1967 to 15 May 1968		
5 AUTHOR(S) (Last name, first name, initial) Kraft, David C.		
6 REPORT DATE July 1968	7a TOTAL NO. OF PAGES 74	7b NO. OF REFS 28
8a CONTRACT OR GRANT NO. AF 33(615)-3199	9a. ORIGINATOR'S REPORT NUMBER(S) None	
b PROJECT NO.	9b. OTHER REPORT NO(S) (Any other numbers that may be assigned this report) AFFDL-TR-68-88	
c.		
d.		
10 AVAILABILITY/LIMITATION/NOTICES This document is subject to special export controls and each transmittal to foreign governments or foreign nationals may be made only with prior approval of the Air Force Flight Dynamics Laboratory (FDFM), Wright-Patterson Air Force Base, Ohio 45433		
11. SUPPLEMENTARY NOTES ↓		12. SPONSORING MILITARY ACTIVITY Air Force Flight Dynamics Laboratory Wright-Patterson Air Force Base, Ohio
13 ABSTRACT The determination of aircraft flotation and operation capability on semi- and unprepared soil runways is a critical factor in developing forward area airfields in limited warfare situations. An investigation was conducted to determine the variables which significantly influence aircraft performance when operating on soil runways. Analysis of available experimental drag-sinkage-velocity data led to the defining of at least three distinct regions for which the sinkage ratio-velocity relationship shows a distinct response. A drag ratio-sinkage ratio equation was developed for use in one of these velocity regions. The effects of twin wheel and tandem wheel arrangements were analyzed on a preliminary basis. The results of a sinkage study using presently available sinkage prediction equations indicated that present sinkage analysis accuracy is in the range of $\pm 50\%$ to $\pm 100\%$. In order to develop a suitable flotation criteria, an investigation was conducted of the dynamic landing gear contacting element-soil interaction response utilizing elastic theory. These results led to the development of a flotation parameter (related to sinkage) and a flotation index (related to drag) in nomographic form which permits comparative flotation analysis of landing gear systems. () This document is subject to special export controls and each transmittal to foreign governments or foreign nationals may be made only with prior approval of the Air Force Flight Dynamics Laboratory (FDFM), Wright-Patterson Air Force Base, Ohio 45433.		

DD FORM 1473
1 JAN 64

Unclassified
Security Classification

14. KEY WORDS	LINK A		LINK B		LINK C	
	ROLE	WT	ROLE	WT	ROLE	WT
Flotation Unprepared soil airfields Drag Sinkage Forward airfields Aircraft operations						

INSTRUCTIONS

1. ORIGINATING ACTIVITY: Enter the name and address of the contractor, subcontractor, grantee, Department of Defense activity or other organization (*corporate author*) issuing the report.

2a. REPORT SECURITY CLASSIFICATION: Enter the overall security classification of the report. Indicate whether "Restricted Data" is included. Marking is to be in accordance with appropriate security regulations.

2b. GROUP: Automatic downgrading is specified in DoD Directive 5200.10 and Armed Forces Industrial Manual. Enter the group number. Also, when applicable, show that optional markings have been used for Group 3 and Group 4 as authorized.

3. REPORT TITLE: Enter the complete report title in all capital letters. Titles in all cases should be unclassified. If a meaningful title cannot be selected without classification, show title classification in all capitals in parenthesis immediately following the title.

4. DESCRIPTIVE NOTES: If appropriate, enter the type of report, e.g., interim, progress, summary, annual, or final. Give the inclusive dates when a specific reporting period is covered.

5. AUTHOR(S): Enter the name(s) of author(s) as shown on or in the report. Enter last name, first name, middle initial. If military, show rank and branch of service. The name of the principal author is an absolute minimum requirement.

6. REPORT DATE: Enter the date of the report as day, month, year; or month, year. If more than one date appears on the report, use date of publication.

7a. TOTAL NUMBER OF PAGES: The total page count should follow normal pagination procedures, i.e., enter the number of pages containing information.

7b. NUMBER OF REFERENCES: Enter the total number of references cited in the report.

8a. CONTRACT OR GRANT NUMBER: If appropriate, enter the applicable number of the contract or grant under which the report was written.

8b, &c, & 8d. PROJECT NUMBER: Enter the appropriate military department identification, such as project number, subproject number, system numbers, task number, etc.

9a. ORIGINATOR'S REPORT NUMBER(S): Enter the official report number by which the document will be identified and controlled by the originating activity. This number must be unique to this report.

9b. OTHER REPORT NUMBER(S): If the report has been assigned any other report numbers (*either by the originator or by the sponsor*), also enter this number(s).

10. AVAILABILITY/LIMITATION NOTICES: Enter any limitations on further dissemination of the report, other than those

imposed by security classification, using standard statements such as:

- (1) "Qualified requesters may obtain copies of this report from DDC."
- (2) "Foreign announcement and dissemination of this report by DDC is not authorized."
- (3) "U. S. Government agencies may obtain copies of this report directly from DDC. Other qualified DDC users shall request through _____."
- (4) "U. S. military agencies may obtain copies of this report directly from DDC. Other qualified users shall request through _____."
- (5) "All distribution of this report is controlled. Qualified DDC users shall request through _____."

If the report has been furnished to the Office of Technical Services, Department of Commerce, for sale to the public, indicate this fact and enter the price, if known.

- 11. SUPPLEMENTARY NOTES:** Use for additional explanatory notes.
- 12. SPONSORING MILITARY ACTIVITY:** Enter the name of the departmental project office or laboratory sponsoring (*paying for*) the research and development. Include address.
- 13. ABSTRACT:** Enter an abstract giving a brief and factual summary of the document indicative of the report, even though it may also appear elsewhere in the body of the technical report. If additional space is required, a continuation sheet shall be attached.

It is highly desirable that the abstract of classified reports be unclassified. Each paragraph of the abstract shall end with an indication of the military security classification of the information in the paragraph, represented as (TS), (S), (C), or (U)

There is no limitation on the length of the abstract. However, the suggested length is from 150 to 225 words.

14. KEY WORDS: Key words are technically meaningful terms or short phrases that characterize a report and may be used as index entries for cataloging the report. Key words must be selected so that no security classification is required. Identifiers, such as equipment model designation, trade name, military project code name, geographic location, may be used as key words but will be followed by an indication of technical context. The assignment of links, rules, and weights is optional.